Water Cycle ~~Acceleration~~ Changes in Czechia: A Multi-Source Water Budget ~~Approach~~Perspective

Mijael Rodrigo Vargas Godoy[1], Yannis Markonis[1], Oldrich Rakovec[2, 1], Michal Jenicek[3], Riya Dutta[1], Rajani Kumar Pradhan[1], Zuzana Bešťáková[1, 4], Jan Kyselý[1, 4], Roman Juras[1], Simon Michael Papalexiou[5, 6, 1], and Martin Hanel[1]

[1]Faculty of Environmental Sciences, Czech University of Life Sciences Prague, Czechia
[2]UFZ-Helmholtz Centre for Environmental Research, Germany
[3]Department of Physical Geography and Geoecology, Charles University, Czechia
[4]Institute of Atmospheric Physics, Czech Academy of Sciences, Czechia
[5]Department of Civil Engineering, University of Calgary, Canada
[6]Global Institute for Water Security, University of Saskatchewan, Canada

Correspondence: M. R. Vargas Godoy (vargas_godoy@fzp.czu.cz)

Abstract. The water cycle in Czechia has been observed to be changing in recent years, with precipitation and evapotranspiration rates exhibiting a trend of acceleration. However, the spatial patterns of such changes remain poorly understood due to the heterogeneous network of ground observations. This study relied on multiple state-of-the-art reanalyses and hydrological modeling. Herein, we propose a novel method for benchmarking hydroclimatic data fusion based on water cycle budget closure. We ranked water cycle budget closure of 96 different combinations for precipitation, evapotranspiration, and runoff using CRU TS v4.06, E-OBS, ERA5-Land, mHM, NCEP/NCAR R1, PREC/L, and TerraClimate. Then, we used the best-ranked data to describe changes in the water cycle in Czechia over the last 60 years. We determined that Czechia is undergoing water cycle acceleration, evinced by increased atmospheric water fluxes. However, the increase in annual total precipitation is not as pronounced nor consistent as evapotranspiration, resulting in an overall decrease in the runoff. Furthermore, non-parametric bootstrapping revealed that only evapotranspiration changes are statistically significant at the annual scale. At higher frequencies, we identified significant spatial heterogeneity when assessing the water cycle budget at a seasonal scale. Interestingly, the most significant temporal changes in Czechia ~~take place~~ occur during spring, while ~~median spatial patterns stem~~ the spatial pattern of the change in median values stems from summer changes in the water cycle, which are the seasons within the months with statistically significant changes.

1 Introduction

During the last decades, there have been significant advances in analyzing the water cycle and its response to global warming. While we expect alterations in the water cycle to respond to climate change and global warming, the actual extent and characteristics of this reaction are poorly understood (Zaitchik et al., 2023). ~~On the one hand, small changes in total precipitation suggest a shift in precipitation towards more intense and less frequent events (Trenberth, 2011). On the other hand, it~~ It was hypothesized that an increased vertical gradient of atmospheric water vapor would offset atmospheric wind convergence in the

tropics making wet regions wetter and dry regions drier (Held and Soden, 2006). Nevertheless, such claims lack conclusive support of observed measurements and have lit the fire of controversy in the field (Vecchi et al., 2006; Allan, 2012; Skliris et al., 2016).

Undoubtedly, the advances in remote sensing observations and process-based modeling have shaped current research the most. However, as the data sources increased, it soon became apparent that large discrepancies between the data sets still exist due to biases and uncertainties (Vargas Godoy et al., 2021). Observational data is hampered by short and heterogeneous ground-based records (Schneider et al., 2017), and unquantified uncertainties on satellite-based products ~~(Sheffield et al., 2009)~~ (e.g., the impact of cloud filtering; Povey and Grainger, 2015). Therefore, reanalysis data providing global coverage through models while assimilating observation-based data has attained an essential role in assessing water cycle changes (Lorenz and Kunstmann, 2012). Each data source has limitations and uncertainties; when multiple sources are combined, these can compound and result in conflicting or unclear results. Hence, in addition to uncertainty due to the complex water cycle system, which involves multiple feedback mechanisms and interactions between different components, we must account for data merge uncertainty. Accordingly, various methodologies for multi-source data integration have emerged. Among the most widely used ones are: Bayesian model averaging, constrained linear regression, neural networks, optimal interpolation, and simple weighting (Rodgers, 2000; Aires, 2014; Moazamnia et al., 2019; Pellet et al., 2019; Xiao et al., 2020). Subsequently, once merged data is generated, it is subject to post-processing for water cycle budget closure via Monte Carlo applications and Kalman filter variations (Pan and Wood, 2006).

Several studies have quantified the water cycle by implementing data integration methods and budget closure constraints, e.g.,: Sahoo et al. (2011) integrated 16 data sets over 10 globally distributed river basins (eight for precipitation, six for evapotranspiration, one for runoff, and one for total water storage); Pan et al. (2012) integrated eight data sets over 32 globally distributed river basins (four for precipitation, two for evapotranspiration, one for runoff, and one for total water storage); Rodell et al. (2015), integrated six data sets over continents and ocean basins (one for precipitation, three for evapotranspiration, one for runoff, and one for total water storage); Zhang et al. (2016), integrated 14 data sets globally (five for precipitation, six for evapotranspiration, one for runoff, and two for total water storage); Munier and Aires (2018) integrated 12 data sets at the global scale (four for precipitation, three for evapotranspiration, one for runoff, and four for total water storage).

The studies mentioned above focus on merging multiple data sets to end up with a single data set per water cycle component at different spatial scales. It is evident that unconstrained uncertainty remains despite the plethora of data products derived from satellites, ground-based measurements, and climate models. This is true even for localized studies at regional scales where "ground-truth" measurements for one or more components of the water cycle are available. One region of particular interest is Czechia, a small country in Central Europe with diverse landscapes and a growing population (United Nations, 2022). The water cycle over Czechia has been experiencing significant changes in recent times, affecting various aspects of the water balance in the region, including changes in river flow regimes and water quality, loss of wetlands, and changes in the frequency and severity of extreme events (Mozny et al., 2020). Besides, changes in the rainfall-snowfall partition have given rise to a decrease in snow cover and premature snowmelt (Nedelcev and Jenicek, 2021). These changes in the water cycle are expected to continue in the near-future (Kyselý and Beranová, 2009; Jenicek et al., 2021). Precipitation, in particular,

is expected to increase its mean mainly in winter and extreme rates throughout the year (Kyselý et al., 2011). In addition, increased human activities, such as urbanization and agriculture, have led to changes in land use and land cover, which in turn has contributed to the occurrence of floods and droughts (Svoboda et al., 2016). Droughts, have had disastrous consequences for agriculture, forestry, water management, and other human activities (Brázdil et al., 2009). Consequently, the water cycle in Czechia and human activity find themselves on a causal feedback loop.

In this study, we aim to estimate the water cycle changes over Czechia between the 1961-1990 and 1991-2020 periods, and determine the current trends and patterns in water cycle components. Our analysis includes various data sets at different spatiotemporal scales allowing us to assess 96 data combinations for budget closure. Rather than enforcing budget closure on a multi-source integrated data set or assessing different integration methods, we explored an empirical method to rank how multiple data set combinations close the water cycle budget while correlating to referential data estimates of individual water cycle components. In this manner, we are not generating yet another new data set but are identifying the best combination among the data sets available for our study domain. Only the data sets with the best rankings as determined by our proposed benchmarking were used in all subsequent computations. We found that hydroclimatic models, as expected, have better water budget closure. However, ERA5-Land is not far off despite known non-closure limitations associated with reanalyses. We identified an overall acceleration of atmospheric water fluxes. Simultaneously, we report a heterogeneous distribution of freshwater availability.

2 Data and Methods

2.1 Study Area

Czechia is a landlocked (surrounded by Germany, Austria, Slovakia, and Poland) European country that covers an area of 78 864 km^2. Czechia is an essential headwaters region of the European continent~~; in hydrological terms, it can be called the roof of Europe~~. The country is home to several large rivers, including the Vltava, the Elbe, the Morava, and the Oder, all of which have their sources within it. Czechia is situated at the intersection of three sea drainage basins: the North Sea, the Baltic Sea, and the Black Sea, which, in return, divide Czechia into three main hydrological catchment areas: the Elbe, Oder, and Danube basins (Figure 1). All of these major watercourses drain water into neighboring states. The water sources of Czechia are thus almost exclusively dependent on precipitation.

2.2 Data

To assess water cycle acceleration we gathered data sets with at least 60 years of record. This first filter reduced the plethora of publicly available data sets to nine data sets from multiple sources (observation-based, reanalysis, and hydrological model products) plus three evaluation references (Table 1). The evaluation data sets for precipitation ~~, evapotranspiration,~~ and runoff are the Czech Hydrometeorological Institute (CHMI)~~, Global Land Evaporation Amsterdam Model (GLEAM v3.6a; Martens et al. (2017)), and GRUN (Ghiggi et al., 2019),~~ and the Global Runoff Data Centre (GRDC), respectively. Six precipitation data sets: Climatic Research Unit at the University of East Anglia (CRU TS v4.06; Harris et al. (2020)), European Centre for Medium-Range

3
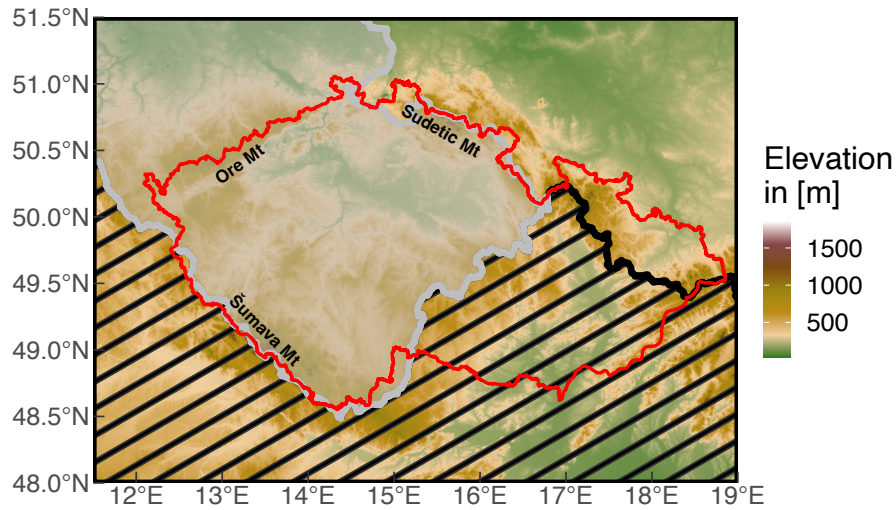
Figure 1. The three drainage basins within Czechia's boundaries. Elbe (light gray shade), Danube (~~dark gray shade~~black stripes), and Oder (~~no shade~~clear).

Weather Forecasts (ECMWF) Reanalysis (ERA5-Land; Muñoz-Sabater et al. (2021)), the E-OBS data set from the Copernicus Climate Change Service (Cornes et al., 2018), National Centers for Environmental Prediction & the National Center for Atmospheric Research Reanalysis One (NCEP/NCAR R1; Kalnay et al. (1996)), Precipitation Reconstruction Over Land (PREC/L; Chen et al. (2002)), and TerraClimate (Abatzoglou et al., 2018). Note that, E-OBS (hereinafter mHM(E-OBS)) was used as meteorologic input for the mesoscale Hydrologic Model (mHM; Samaniego et al. (2010); Kumar et al. (2013)). Four evapotranspiration data sets: ERA5-Land, mHM, NCEP/NCAR R1, and TerraClimate. Four runoff data sets: ERA5-Land, mHM, NCEP/NCAR R1, and TerraClimate. Using the above listed data sets we assessed a total of 96 different combinations.

Table 1. Data set description. P is precipitation, E is evapotranspiration, and Q is runoff.

Name	Variable(s)	Spatial Resolution	Temporal Resolution	Record Length	Data Type
CHMI	P	Point	Daily	1961-2020	Stations
CRU TS v4.06	P	1°	Monthly	1901-2020	Gauge-based
E-OBS	P	0.125°	Daily	1950-2020	Gauge-based
ERA5-Land	P, E, Q	0.1°	Monthly	1950-2020	Reanalysis
~~GLEAM v3.6a~~ GRDC	~~E~~ Q	~~0.25°~~ Point	Daily	~~1980-2020~~ 1921-2017	~~Martens et al. (2017)~~GRUN Station
mHM	E, Q	0.125°	Daily	1950-2020	Model
NCEP/NCAR R1	P, E, Q	T62	Monthly	1948-2020	Reanalysis
PREC/L	P	0.5°	Monthly	1948-2020	Gauge-based
TerraClimate	P, E, Q	4 km	Monthly	1958-2020	Model

4

2.2.1 Evaluation References

95 The Czech Hydrometeorological Institute (CHMI) provides station derived precipitation data. The CHMI station network consists of approximately 700 stations distributed with a mean density of one station per each $100 \, \text{km}^2$, adequately representing the distinct geographical features of Czechia (Kašpar et al., 2021). Although the data collection and related services for a specific station are generally managed by the regional branches of CHMI, the entire territory station data can be accessed from the Department of Climatology of CHMI at once. All the data sets are undergone robust quality control checks by CHMI before

100 being added to the database. Herein, we gathered the country level estimates calculated by CHMI (one value per month) for a period of 60 years (1961-2020).

The Global ~~Land Evaporation Amsterdam Model (GLEAM~~Runoff Data Centre (GRDC) is a ~~satellite-based global evaporative model designed to estimate terrestrial evapotranspiration from 1980 to the near present (Martens et al., 2017). It encompasses a set of algorithms that estimates a total of 11 variables, including actual and potential evapotranspiration rates. Briefly, the~~

105 ~~estimation procedure consists of two major steps. First, given the temperature and radiation data sets, potential evapotranspiration rates in mm/dayare estimated by land cover type using the Priestley and Taylor equation (Priestley and Taylor, 1972). Second, potential evapotranspiration is converted into actual evapotranspiration based on an evaporative stress factor. Despite GLEAM not being a ground station derived product, or even a fully observation-based data set, previous studies have extensively evaluated GLEAM and advocate for its high quality (Yang et al., 2017; Bai and Liu, 2018; Liu et al., 2021).~~

110 ~~GRUN is a gridded global monthly runoff reconstruction generated by a machine learning model (Ghiggi et al., 2019). It is available at a 0.5° spatial resolution~~ collection of river discharge data from more than 8000 stations in 157 countries. The GRDC operates under the the World Meteorological Organization (WMO) since 1988 to collect, manage, and distribute data related to river discharge and runoff from around the world. The data collected at GRDC undergoes quality control to check for errors, inconsistencies, and outliers in the data before its dissemination. While data is available at daily and monthly time

115 step~~from 1902 to 2014. Conceptually, the machine learning algorithm was trained with observations of monthly temperature, precipitation and streamflow. Then, the trained model is used to predict monthly runoff at ungauged catchments. Although the method does not implement any physically detailed hydrological model, the predicted runoff showed better results than the ensemble mean of 13 global hydrological model simulations when compared to observational references. Furthermore, GRUN has been extensively applied in regions with sparse in-situ measurements (Hu et al., 2021; Xiong et al., 2022; Xu et al., 2022; Mei et al., 20~~

120 ~~.~~, the record length varies by location. We selected three stations from GRDC, namely the Bohumin (Oder), Decin (Elbe), and Moravsky Jan (Danube) stations, which are placed near the borders of the country and country level estimates were calculated by their wieighted average based the catchment area as registered by GRDC.

2.2.2 Observational-based Products

CRU TS is a popularly used gridded data set generated by the University of East Anglia's Climate Research Unit (Harris

125 et al., 2020). It is known for its historical long-term coverage, which is available from 1901 to the near present. The data set comes with a 0.5° spatial resolution at the monthly scale. It compiles station data from multiple sources such as the Food and

Agricultural Organisation (FAO), the World Meteorological Organisation (WMO), and the National Meteorological Agencies (NMA's) (Sun et al., 2018). CRU TS v4, its latest version, implemented angular distance based interpolation to facilitate tracing back the stations upon which the gridded data set has been constructed.

130   PREC/L, created by the US Climate Prediction Center (CPC), is a gridded product entirely based on the station data set (Chen et al., 2002) with global coverage and monthly time step. PREC/L draws data from over 17 000 stations from the Global Historical Climatology Network version2 (GHCN v2; Peterson and Vose, 1997) and the Climate Anomaly Monitoring System (CAMS; Janowiak and Xie, 1999). Subsequently, the data is interpolated to construct the gridded product at three different resolutions (0.5°, 1°, and 2.5°). Herein, we used the 0.5° monthly precipitation, whose record extends from 1948 to

135   the present.

2.2.3   Hydrological Models

The mesoscale Hydrologic Model (mHM; Samaniego et al., 2010; Kumar et al., 2013) is a conceptual grid-based model representing dominant hydrological fluxes and storage at the Earth's surface and subsurface through a ~~set~~ system of ordinary differential equations. mHM represents processes such as interception, snow, soil moisture, evapotranspiration, and various

140   runoff components like fast/slow interflow and baseflow. The model was established, parameterized and evaluated over the European continent (Rakovec et al., 2016b; Samaniego et al., 2019; Rakovec et al., 2022). The meteorological inputs were based on daily E-OBS data (Cornes et al., 2018) of precipitation in addition to minimum, maximum and average temperature. The potential evapotranspiration was derived using the method of (Hargreaves and Samani, 1982). The spatial resolution of the model grid corresponds to 0.125°.

145   Terraclimate is a high-resolution gridded global climate data set that provides the mean climate and mean water balance data covering a time span of 1958 to the present (Abatzoglou et al., 2018). The data set is commonly known for its high spatial resolution (4 km). It uses various global gridded climate data sets such as WorldClim v2 (Fick and Hijmans, 2017) and v1.4 (Hijmans et al., 2005), CRU TS v4 (Harris et al., 2020), Japanese 55-year Reanalysis (JRA55) (Kobayashi et al., 2015), and Root zone storage capacity (Wang-Erlandsson et al., 2016) in order to generate the high-resolution monthly climate variables

150   time series at the global level. An additional advantage of the Terraclimate is that it produces monthly surface water balance based on a water balance model along with primary climatic variables such as temperature, precipitation, solar radiation, etc.

2.2.4   Reanalyses

ERA5-Land is the latest fifth-generation global atmospheric reanalysis product developed by the European Center for Medium-Range Weather Forecast (ECMWF) (Muñoz-Sabater et al., 2021). ERA5-Land, as the name implies, builds upon the terrestrial

155   component of ERA5 and downscales the model spatial grid resolution from 31 km into 9 km. As a result, ERA5-Land delivers either hourly or monthly estimates with a spatial resolution of 0.1°. Given its high spatiotemporal resolution and long record, ERA5-Land provides valuable data for comprehensive analysis and diverse hydrological applications at the global scale.

The NCEP/NCAR Reanalysis project one is produced by the collaboration between the National Centers for Environmental Prediction (NCEP) and the National Center for Atmospheric Research (NCAR) (Kalnay et al., 1996). It is the longest-running

reanalysis that uses rawindsonde data, at the expense that the model and data assimilation scheme are antiquated Trenberth et al. (2011). The data set is distributed on a T62 Gaussian grid (approximately $1.875°$ at the equator) and its record start dates back to 1948.

2.3 Data Evaluation

We validated the gathered data sets to capture the temporal variability of water cycle components as described by the three observational references via ~~: The~~ the coefficient of determination (R-squared or R^2)

$$R^2 = 1 - \frac{\sum_i^n (y_i - \hat{y}_i)^2}{\sum_i^n (y_i - \overline{y})^2}$$

~~where i starts on the first year of the available record, n is the last year of the available record, y_i is the observational reference on year i, $\hat{y}_i$ is the data set estimate on year i, and $\overline{y}$ is the mean observational estimate for the full available record.~~ and the Root Mean Square Error (RMSE)

$$\text{RMSE} = \sqrt{\frac{\sum_i^n (y_i - \hat{y}_i)^2}{N}}$$

~~where i starts on the first year of the available record, n is the last year of the available record, y_i is the observational reference on year i, $\hat{y}_i$ is the data set estimate on year i, and N is the total number of years in the full available record.~~

All data sets were spatial weighted averaged over Czechia and temporally aggregated to an annual scale over the calendar year. Note that only precipitation data sets could be evaluated over the entire 60-year period of 1961-2020. In contrast, ~~evapotranspiration~~ runoff was evaluated over ~~1980-2020 and runoff over 1961-2014~~ 1961-2017. In order to compare a 30-year mean among all water cycle components, the common period of 1981-2010 was selected.

2.4 Data Set Ranking

A success metric widely used among several studies is getting the budget closure residual (~~R~~ξ) as close to zero as possible. Herein, we define the budget closure residual as follows:

$$R\xi_n = P_n - E_n - Q_n \tag{1}$$

~~where P~~

where P_n is precipitation, ~~E~~ E_n is evapotranspiration, and ~~Q is runoff~~ Q_n is runoff for a given year n. Thus, we have ~~96 distributions of~~ 60 annual values ~~each. The~~ for each of the 96 possible combinations. Under steady state conditions the mean of these residuals should tend to zero:

$$\overline{\xi_i} = \frac{\sum_{n=1}^N \xi_n}{N} \to 0 \tag{2}$$

7

where $\overline{\xi_i}$ is the mean of the $N = 60$ annual residuals for the i-th combination. The score to be used in the ranking of a given data set combination was determined via:

$$Ranking score = \frac{|\overline{R_i}|\sigma_{R_i}}{(cor(P_i - E_i, Q_i)cor(P_i, P_o)cor(E_i, E_o)cor(Q_i, Q_o))^2} \frac{|\overline{\xi_i}|\sigma_{\xi_i}}{(cor(P_i - E_i, Q_i)cor(P_i, P_o)cor(E_i, E_o)cor(Q_i, Q_o))^2}$$

(3)

where $|\overline{R_i}|$

190 where $|\overline{\xi_i}|$ is the absolute value of the mean of the 60 annual residuals for the i-th combination, σ_{R_i} σ_{ξ_i} is the standard deviation of the 60 annual residuals for the i-th combination, $cor(P_i - E_i, Q_i)$ is the correlation between $P - E$ and Q for the i-th combination, $cor(P_i, P_o)$ is the correlation between P of the i-th combination and the precipitation evaluation reference, $cor(E_i, E_o)$ is the correlation between E of the i-th combination and the evapotranspiration evaluation reference, and $cor(Q_i, Q_o)$ is the correlation between Q of the i-th combination and the runoff evaluation reference. zzzz The ranking method

195 proposed herein can easily be applied to any other referential data set for evaluation. In data-limited areas or those with a poor observational network, the ranking method may still be applied using external data as an evaluation reference, or the corresponding term in the equation can be simply left out. E.g., if evapotranspiration data for evaluation is not available, Equation 3 becomes:

$$Ranking = \frac{|\overline{R_i}|\sigma_{R_i}}{(cor(P_i - E_i, Q_i)cor(P_i, P_o)cor(Q_i, Q_o))^2}$$

200 $$score = \frac{|\overline{\xi_i}|\sigma_{\xi_i}}{(cor(P_i - E_i, Q_i)cor(P_i, P_o)cor(Q_i, Q_o))^2}$$

In the case of Czechia, we used GLEAM v3.6a as the evaluation reference, this modified version due to the absence of access to observational evapotranspiration data.

2.5 Water Cycle Changes

We assessed the empirical distribution of spatial weighted average values (accounting for the area of each grid cell in proportion

205 to the total area being averaged) of annual water cycle fluxes between 1961-1990 and 1991-2020 for three of the best data set combinations. To account for the influence of extreme value in the latter period due to the 100-year drought of 2003 (Brázdil et al., 2013), we compared the median values rather than their means (see Figure 5). To deepen our assessment of changes in the distribution of water cycle fluxes, we compared their monthly values between 1961-1990 and 1991-2020. To determine the statistical significance of the above-mentioned changes, we employed non-parametric bootstrapping of 10 000 iterations.

210 Subsequently, we performed an analogous analysis in space. We computed the change in the median values between 1961-1990 and 1991-2020 over each grid cell. Note that each data set was assessed at its native resolution for this part of the analysis.

Finally, we examined the change patterns of water cycles through the seasons. Herein, we considered: winter as December, January, and February; spring as March, April, and May; summer as June, July, and August; autumn as September, October, and November.

## 3 Results

3.1 Benchmarking water cycle components

Our analysis describes the most recent spatiotemporal changes on the water cycle in Czechia. For starters, we examined precipitation, evapotranspiration, and runoff estimates from the gathered data sets. Further, precipitation and runoff were compared to CHMI (Figure 2a) ~~, GLEAM v3.6a (Figure 2b), and GRUN v1~~ and GRDC (Figure 2c) as the respective evaluation references. The variability of estimates from precipitaion and runoff data sets (Figure 2a and c) visibly have a broader spread than those of evapotranspiration (Figure 2b). While one may suspect the spread in precipitation is due to the higher number of data sets available, they correlate better to their evaluation reference than ~~evapotranspiration or~~ runoff. The data set with the highest correlation values for precipitation is mHM(E-OBS) with R-squared of approximately 0.99 (Figure 2a). mHM has the highest correlation for runoff, with R-squared circa ~~0.86~~ 0.93 (Figure 2c)~~, falling to the second highest for evapotranspiration (R-squared 0.7; Figure 2c). Interestingly, the values for the 30-year average in mHM underestimates runoff (Figure 2c) but overestimates evapotranspiration (Figure 2b).~~ In contrast, NCEP/NCAR R1 consistently reports the lowest correlation values regardless of the water flux of interest. Additionally ~~, other than for runoff, it has considerably~~ it has substantially higher RMSE values than the rest of the data sets for precipitation. To some degree, ERA5-Land is the in-betweener data set because it has high correlation values and simultaneously has high RMSE for precipitation~~and evapotranspiration~~, yet for runoff, ERA5-Land exhibits moderate correlation and small RMSE.

The water cycle budget is meant to close over hydrological units. Accordingly, we examined the water fluxes of the data sets with the best evaluation over the subbasins enclosed by the Czech administrative borders (Figure 3). For simplicity, we will refer to them by their river names inside Czechia. I.e., Morava for the Danube basin, Labe for the Elbe basin, and the Odra for the Oder basin. It can be seen that within each data set, no extremely deviant behavior is exhibited between basins or at the country level. In other words, the precipitation time series depicted by TerraClimate for Czechia is similar to the one depicted for the Morava, Labe, and Odra Rivers. Comparing data sets, however, it is evident that ERA5-Land is different. At first glance, we evince higher magnitudes for ERA5-Land precipitation and evapotranspiration, yet the residuals do not appear to be that far off from those of mHM or TerraClimate. It is not until we look at the cumulative sum of the residuals that we can distinguish ERA5-Land water budget residuals are nonstationary with a decreasing trend.

It would be sensible to use the best data set for each water flux to proceed with further analysis. However, we first verified if the best data sets individually would depict the best water cycle budget in conjunction. Conventional metrics like R-squared and RMSE cannot be directly applied to a combination of data sets. We defined an empirical ~~ranking~~ scoring metric, as described by Equation 3, where the smallest the value, the better the data set combination. While our ranking approach is empirical and simple, Equation 3 correctly identifies narrow distribution centered mean zero with higher ranked positions compared to wider
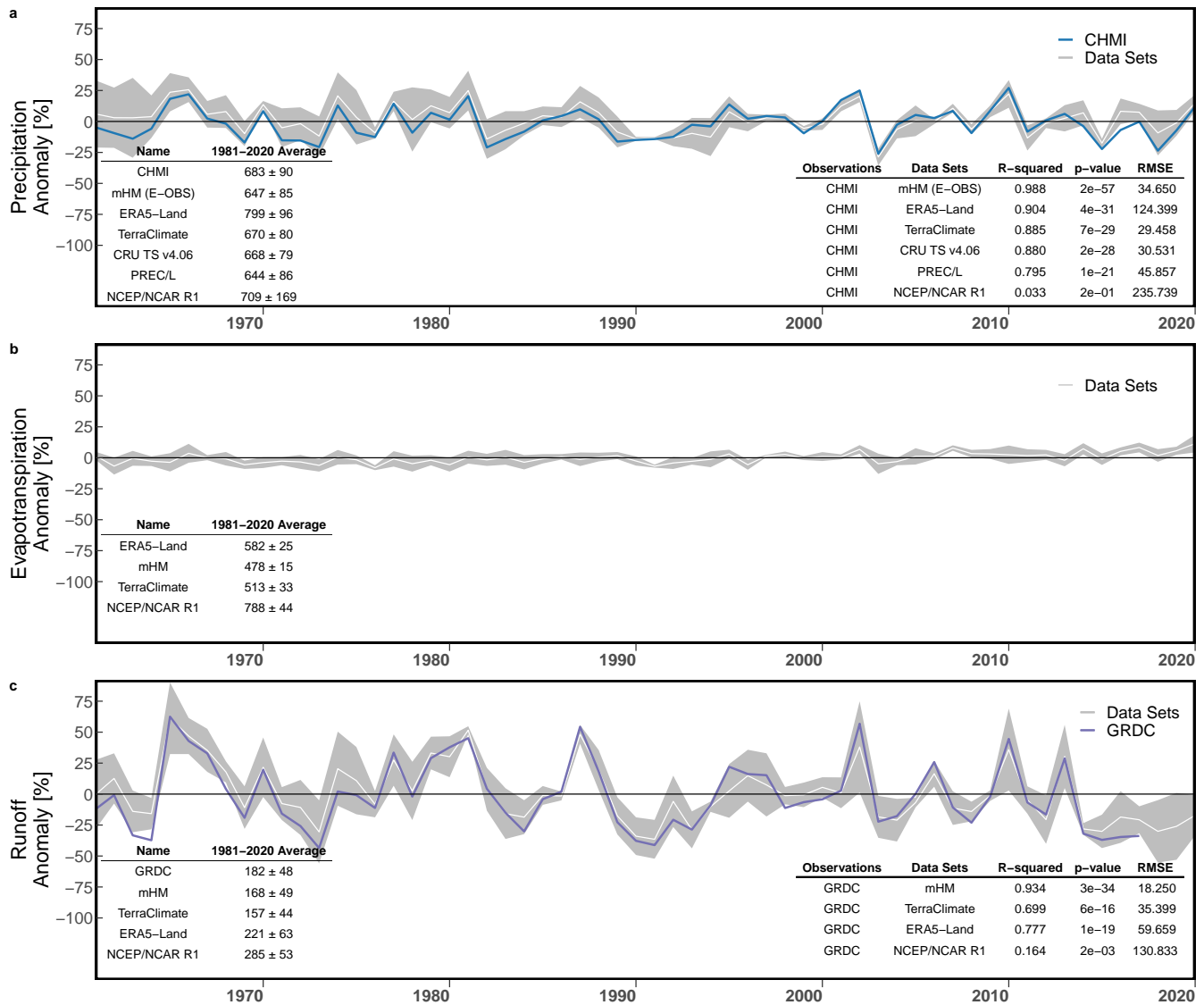
Figure 2. Benchmarking spatial weighted average annual water fluxes over Czechia between 1961 and 2020. For consistency and comparability between different water fluxes, annual anomalies were computed using the 1981-2010 average as a reference, the common period among all data sets. The 1981-2010 average and standard deviation are listed at the bottom left of each panel. Linear correlation summary statistics are displayed at the bottom right of each panel. The spread of the estimates being evaluated is shown in gray, and their mean is in white. (a) Precipitation evaluation. CHMI data is shown in blue. (b) Evapotranspiration evaluation. ~~GLEAM v3.6a is shown in green.~~ (c) Runoff evaluation. ~~GRUN v1~~ GRDC data is shown in purple.

10
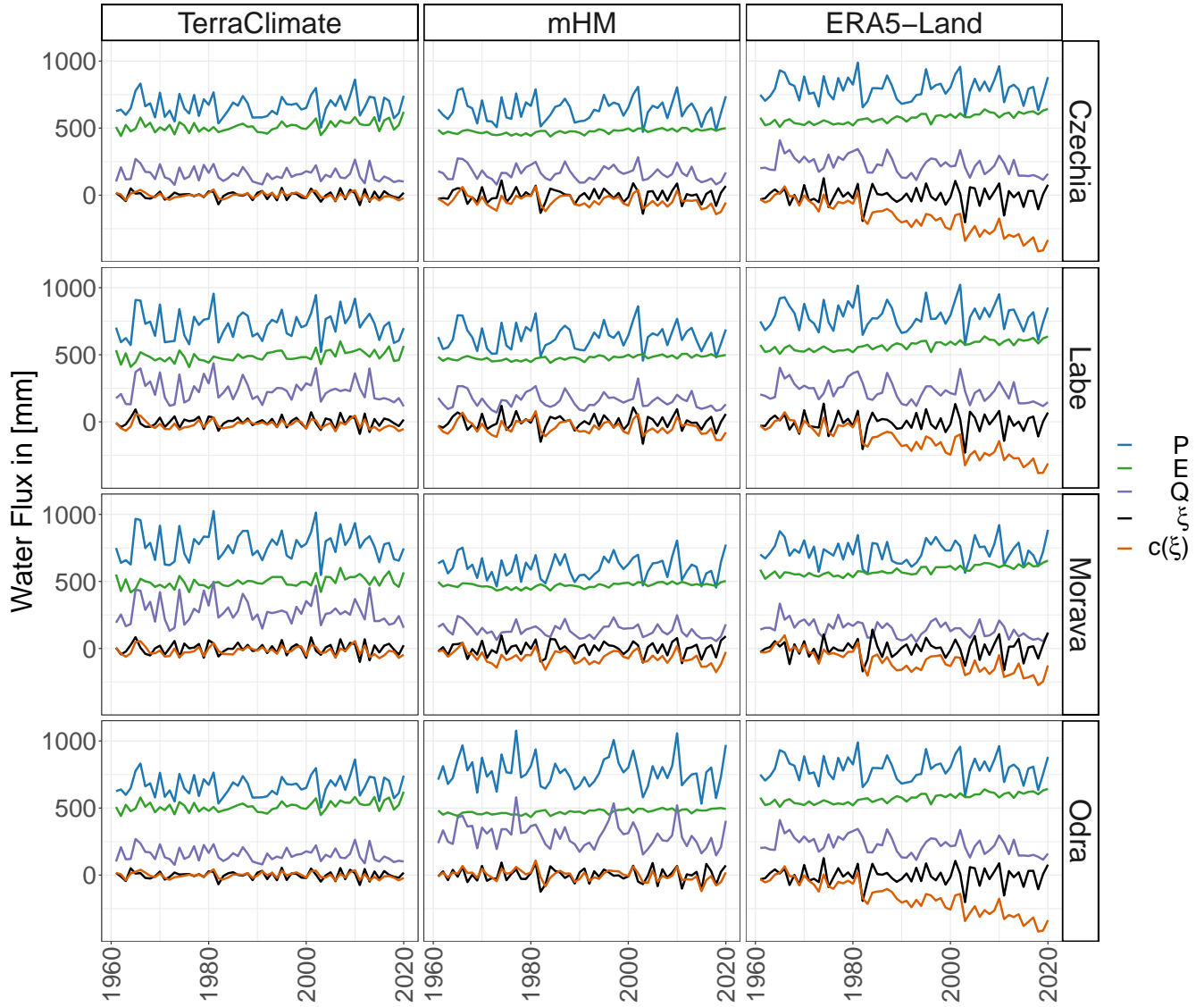
Figure 3. Spatial weighted average annual water fluxes over Czechia (first row), Labe River (Elbe basin inside Czechia; second row), Morava River (Danube basin inside Czechia; third row), and Odra River (Oder basin inside Czechia; fourth row). Where P is precipitation in blue, E is evapotranspiration in green, Q is runoff in purple, ξ is the residual ($P - E - Q$) in black, and c(ξ) is the cumulative sum of the residual in orange. Left column: TerraClimate (P), TerraClimate (E), and TerraClimate (Q). Middle column: mHM(E-OBS) (P), mHM (E), and mHM (Q). Right column: ERA5-Land (P), ERA5-Land (E), and ERA5-Land (Q).

245 distributions centered around positive or negative values (Figure 4). Upon ranking all 96 possible combinations (Table 2), we observe that even though mHM outperformed TerraClimate for individual water flux estimates, the TerraClimate exclusive combination offers the best water budget closure. We expected combinations with hydrological model data to be highly ranked and reanalyses to be poorly ranked due to the above-reported considerable biases of the latter. Notwithstanding, we were surprised to see the ERA5-Land exclusive combination (i.e., all flux estimates from the same data set) among the top ~~five ranks~~

250 six ranks despite non steady water budget residuals (Figure 3) as well as biases 1.7-3.3 and 3.8-4.2 times larger than those of models for runoff (Figure 2c) and precipitation (Figure 2a), respectively. The first combination that includes at least one estimate from NCEP/NCAR R1 is at the ~~45th~~ 38th rank, and the NCEP/NCAR R1 exclusive combination is at the ~~90th~~ 87th rank.
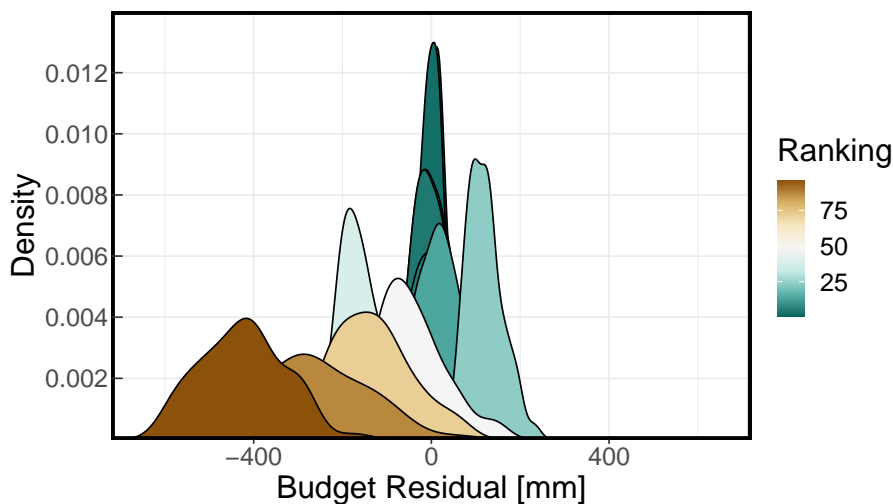
Figure 4. Empirical distribution of ~~all possible 96~~ the data set combinations listed on Table 2 colored based on their ranking as determined by Equation 3. The color gradient goes from higher ranked combinations colored in shades green to lower ranked combinations colored in shades of brown.

3.2 Temporal changes in the water cycle

255 Moving forward, we computed the change in water fluxes' annual distribution via shifts on their 30-year median (Figure 5). Also, we assessed the statistical significance of the observed change in the medians by non-parametric bootstrapping (10 000 iterations). Hereupon, we will report results only for the first- (TerraClimate exclusive), second- (mHM exclusive), and ~~fifth-ranked~~ sixth-ranked (ERA5-Land exclusive) data combinations. Because the third- (CRU TS v4.06, TerraClimate, Ter-raclimate)~~and fourth-ranked (mHM, mHM, TerraClimate~~fourth- (TerraClimate, TerraClimate, mHM), and fifth-ranked (CRU

260 TS v4.06, TerraClimate, mHM) data combinations have a single data set different from the first- and second-ranked ones, as such, we would be showing the same plots and statistics multiple times. TerraClimate and mHM show similar increases in precipitation and evapotranspiration circa 20 mm, but only evapotranspiration manifests a statistically significant change (p

Table 2. Data set ranking as determined by Equation 3. P is precipitation, E is evapotranspiration, Q is runoff, ~~$\bar{R}$~~ $\bar{\xi}$ is the mean residual over 60 years, ~~σ_R~~ σ_ξ is the standard deviation of the residual over 60 years, $cor(P-E,Q)$ is the correlation between $P-E$ and Q for the i-th ranked combination, $cor(P,P_o)$ is the correlation between P of the i-th ranked combination and CHMI, ~~$cor(E,E_o)$ is the correlation between E of the i-th ranked combination~~ and ~~GLEAM v3.6a, and~~ $cor(Q,Q_o)$ is the correlation between Q of the i-th ranked combination and ~~GRUN v1~~ GRDC.

Ranking	P	E	Q	~~$\bar{R}$~~ $\bar{\xi}$	~~σ_R~~ σ_ξ	$cor(P$
1st	TerraClimate	TerraClimate	TerraClimate	-0.346	30.204	
2nd	mHM(E-OBS)	mHM	mHM	-0.912	51.231	
3rd	CRU TS v4.06	TerraClimate	TerraClimate	-1.749	29.944	
4th	~~mHM(E-OBS)~~ TerraClimate	~~mHM~~ TerraClimate	~~7.604~~ mHM	~~56.406~~ -8.861	~~0.754~~ 39.847	~~0.99~~
5th	~~ERA5-Land~~ CRU TS v4.06	~~ERA5-Land~~ TerraClimate	~~ERA5-Land~~ mHM	~~-5.554~~ -10.265	~~66.606~~ 40.613	~~0.70~~
6th	~~PREC/L~~ ERA5-Land	~~mHM~~ ERA5-Land	~~mHM~~ ERA5-Land	~~8.498~~ -5.554	~~61.887~~ 66.606	~~0.63~~
⋮	⋮	⋮	⋮	⋮	⋮	
~~11th~~ 14th	PRECL/L	mHM	TerraClimate	17.013	60.281	
⋮	⋮	⋮	⋮	⋮	⋮	
24th	ERA5-Land	~~ERA5-Land~~ TerraClimate	~~64.008~~ mHM	~~65.157~~ 114.628	~~0.748~~ 44.721	
⋮	⋮	⋮	⋮	⋮	⋮	
~~45th~~ 38th	ERA5-Land	NCEP/NCAR R1	~~ERA5-Land~~ mHM	~~ERA5-Land~~ -166.746	~~2.3~~ 60.420	~~193.9~~
⋮	⋮	⋮	⋮	⋮	⋮	
48th	PREC/L	~~TerraClimate~~ mHM	ERA5-Land	~~-91.688~~ -52.549	~~61.887~~ 82.751	~~0.41~~
⋮	⋮	⋮	⋮	⋮	⋮	
72nd	mHM(E-OBS)	mHM	NCEP/NCAR R1	~~TerraClimate~~ -134.044	~~-312.910~~ 87.923	~~59.1~~
⋮	⋮	⋮	⋮	⋮	⋮	
~~90th~~ 87th	NCEP/NCAR R1	NCEP/NCAR R1	NCEP/NCAR R1	~~292.024~~ -292.024	137.297	
⋮	⋮	⋮	⋮	⋮	⋮	
96th	CRU TS v4.06	NCEP/NCAR R1	NCEP/NCAR R1	-424.772	93.962	

< 0.01). Evapotranspiration changes underwhelming those of precipitation stand further accentuated in ERA5-Land, whose magnitude of the change in evapotranspiration is almost 60 mm and in precipitation is less than -1 mm. Another peculiarity of

265 ERA5-Land is that runoff, with a change of -56 mm at p = 0.01 statistical significance. Regarding the estimates for precipitation minus evapotranspiration, we observe three different behaviors: TerraClimate has a change in P-E in the opposite direction of runoff (1 mm vs. -5 mm); mHM has a change in P-E of smaller magnitude than runoff (-2 mm vs. -9 mm); ERA5-Land has similar changes for both P-E and runoff (-55 mm vs. -56 mm), but with values one order of magnitude higher than those of TerraClimate and mHM.
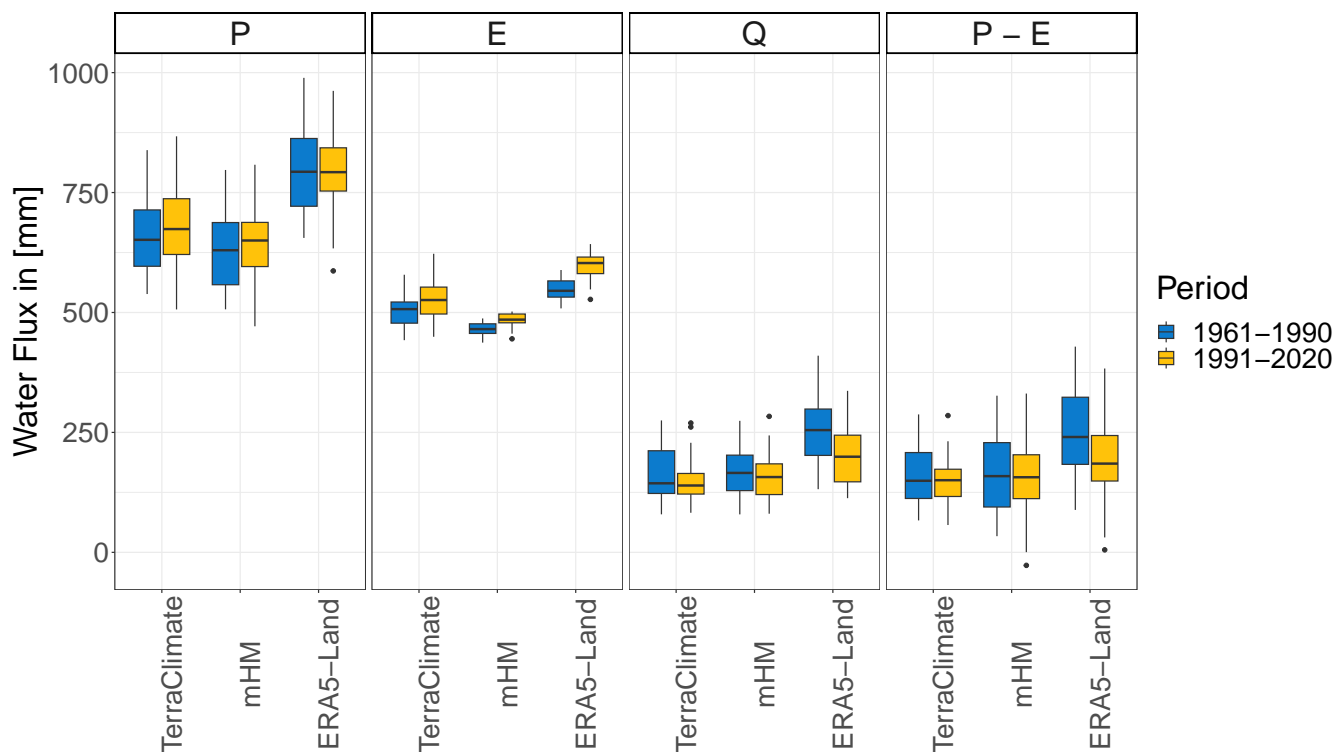
Figure 5. ~~Histograms~~ Box plots of spatial weighted average annual water fluxes over Czechia, where P is precipitation, E is evapotranspiration, Q is runoff, and $P - E$ is precipitation minus evapotranspiration. Data are divided into two 30-year periods: 1961-1990 (~~light gray~~blue) and 1991-2020 (~~dark gray~~yellow). ~~The median value of each 30-year period is represented by dashed lines~~ Note that outliers are present only in ~~their respective color. Top row: TerraClimate~~ the latter period (P)i.e., ~~TerraClimate (E~~1991-2020) ~~, and TerraClimate (Q). Middle row:~~ ~~mHM(E-OBS) (P), mHM (E), and mHM (Q). Bottom row: ERA5-Land (P), ERA5-Land (E), and ERA5-Land (Q).~~as expected from the recorded severe drought of 2003.

270 The above results, seemingly disagreeing with the expected increases reported in previous literature (Kyselý and Beranová, 2009; Svoboda et al., 2016; Kašpárek and Kožín, 2022), indicate that there have not been any statistically significant changes in median annual precipitation over Czechia between the last two 30-year periods. Thereafter, we proceeded to look into

14

changes between 1961-1990 and 1991-2020 monthly water fluxes (Figure 6). Note that hereinafter we mention only months with statistically significant changes (p < 0.01). Regarding precipitation, we observe a consistent increase of around 14 mm

275 during October and circa 11 mm during July present in TerraClimate, mHM(E-OBS), and ERA5-Land. Besides, mHM(E-OBS) and ERA5-Land had decreasing changes in April of -6 mm and -9 mm, respectively. We also found a -5 mm decrease during November, present only in mHM(E-OBS). In terms of evapotranspiration, as expected from the statistically significant changes described for annual values, we report increases between 1-10 mm depending on the month. TerraClimate has the shortest period of continuous changes with gradually increasing magnitude from January (1 mm) to March(9 mm). mHM on top of

280 said evapotranspiration behavior from January (1 mm) to April (4 mm) also shows the subsequent oscillating behavior: May (2 mm), June (2 mm), July(4 mm), and August (3 mm). ERA5-Land changes in evapotranspiration have a behavior similar to mHM but with overall higher magnitudes and two months longer. I.e., a consecutive increase from December (1 mm) to April (8 mm) and subsequent swings back and forth: May (7 mm), June (7 mm), July(10 mm), August (8 mm), and September (3 mm). Concerning runoff, there is a striking unique visual for TerraClimate, whose range of values from February to ~~Abril~~

285 April is considerably larger than those of mHM or ERA5-Land. A runoff decrease is present in all data sets for April and May, with an added magnitude of -18 mm, -8 mm, and -12 mm for TerraClimate, mHM, and ERA5-Land, respectively. Interestingly, these runoff decreases are translated only into mHM and ERA5-Land through precipitation minus evapotranspiration decrease in April (-6 mm and -15 mm).

### 3.3 Spatial patterns of water cycle changes

290 The results shown so far provide insight into the temporal changes water cycle components have undergone in the past 60 years, considering spatial weighted averaged values across Czechia. To expand our analysis from the temporal into the spatial domain and provide insight into the spatiotemporal features of the selected data sets, we mapped the difference between the 1991-2020 and the 1961-1990 medians for P, E, Q, and $P - E$ (Figure 7). Note that maps for each product were generated at their native resolutions, i.e., TerraClimate at 4 km, mHM at 0.125°, and ERA5-Land at 0.1°. At first glance, we observe

295 overall agreement in spatial patterns between data sets for evapotranspiration and runoff, with slight discrepancies around the Sudetic (northeast), Šumava (southwest), and Ore (northwest) Mountains. In particular, ERA5-Land exhibits changes of higher magnitude in evapotranspiration (increase) and runoff (decrease) than TerraClimate and mHM.

Contrary to the above-described agreement, there is no consensus on spatial precipitation patterns among data sets. We discern three different patterns: TerraClimate shows a homogeneous increase across the country with a particular contour of

300 higher increase that starts at the Šumava Mountains and diminishes toward the Ore Mountains and a slight decrease around the Sudetes; ERA5-Land portrays a somewhat zonal pattern with increasing bands north of 50.5°N and south of 49.5°N of the country and a decreasing band in the middle; mHM pattern is in between those of TerraClimate and ERA5-Land, with the band of precipitation decrease being smaller than that of ERA5-Land confined west of 15°E. While some of these heterogeneities are echoed in $P - E$ spatial patterns, there is a general decrease across data sets over Czechia. Therefore, evapotranspiration

305 changes appear to dominate the spatial distribution of water availability.

15
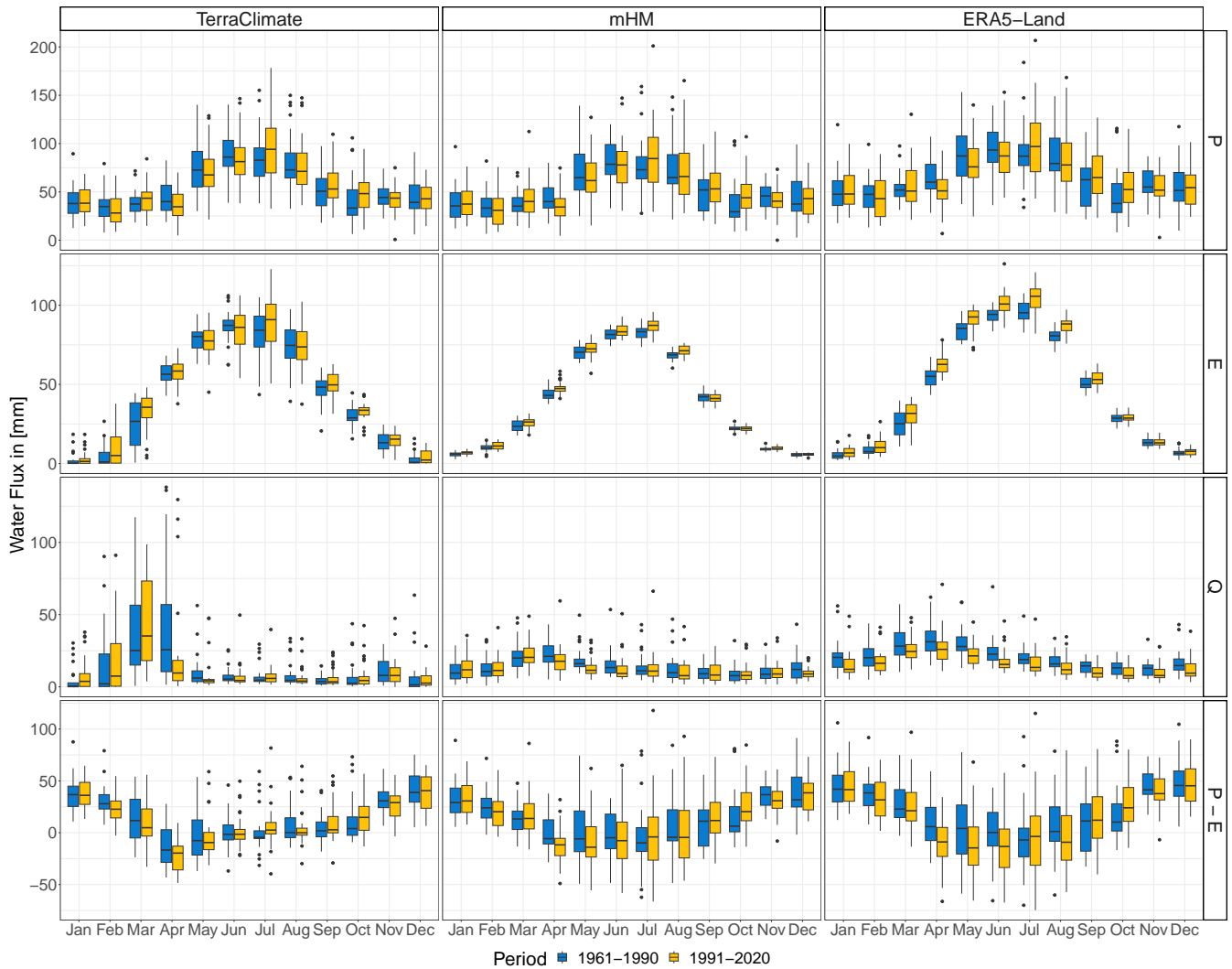
Figure 6. Box plot of spatial weighted average monthly water fluxes over Czechia, where P is precipitation, E is evapotranspiration, Q is runoff, and $P - E$ is precipitation minus evapotranspiration. Data are divided into two 30-year periods: 1961-1990 (light gray blue) and 1991-2020 (dark gray yellow). Left column: TerraClimate (P), TerraClimate (E), and TerraClimate (Q). Middle column: mHM(E-OBS) (P), mHM (E), and mHM (Q). Right column: ERA5-Land (P), ERA5-Land (E), and ERA5-Land (Q).
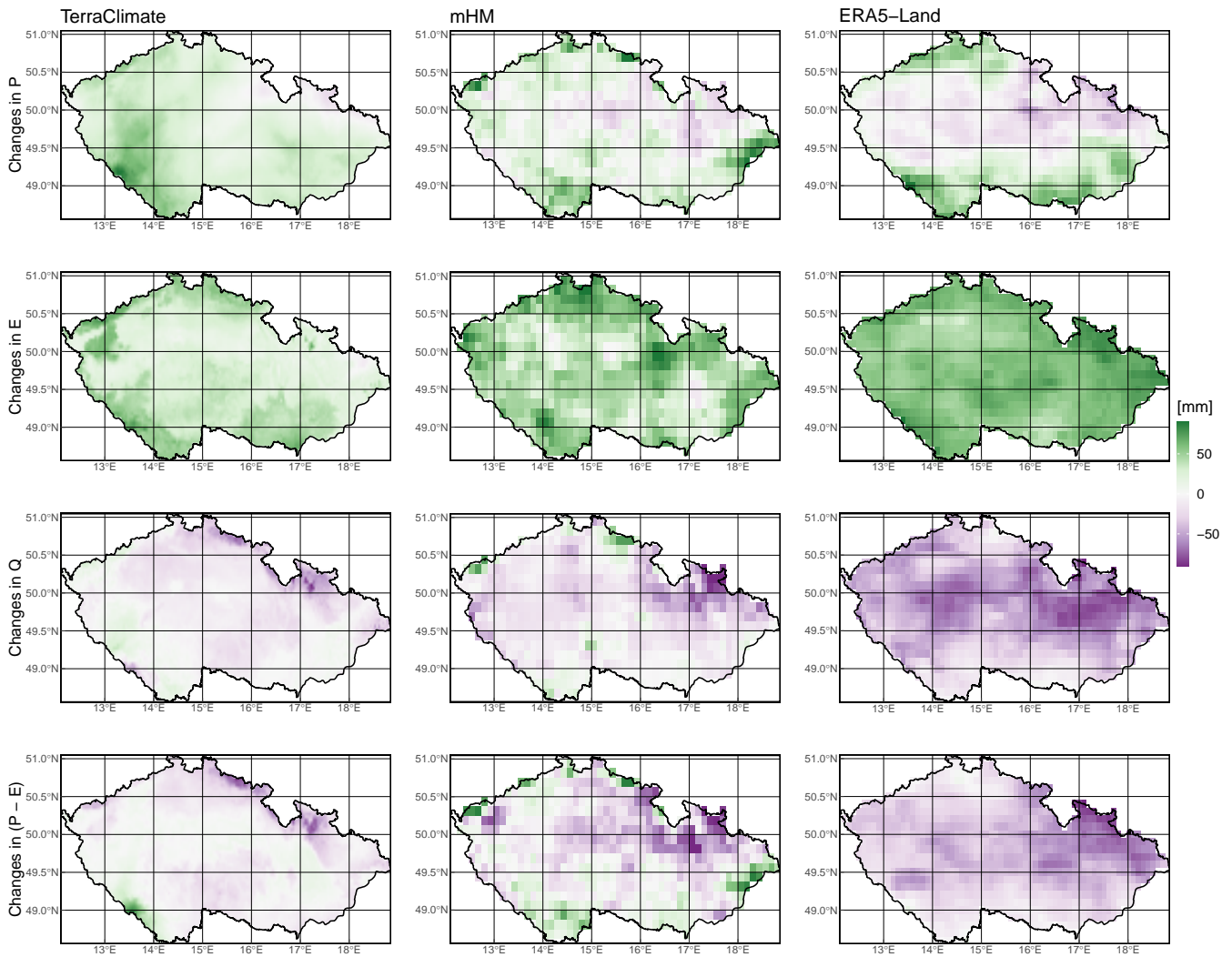
Figure 7. Spatial pattern of changes in median water fluxes over Czechia between two 30-year periods: 1961-1990 and 1991-2020. I.e., the value of each grid cell is equal to the median value of 1991-2020 minus the median value of 1961-1990. P is precipitation, E is evapotranspiration, Q is runoff, and $P - E$ is precipitation minus evapotranspiration. Left column: TerraClimate (P), TerraClimate (E), and TerraClimate (Q). Middle column: mHM(E-OBS) (P), mHM (E), and mHM (Q). Right column: ERA5-Land (P), ERA5-Land (E), and ERA5-Land (Q).

Based on the results observed in Figure 6, we have previously identified that monthly patterns of increase or decrease in water fluxes are, to some extent, aligned with their seasonal variability. Thus this time around, we aggregated the data seasonally rather than looking at the monthly spatial distribution of changes in the median between the two 30-year periods. While individual characteristics for each data set are further emphasized by looking into seasonal spatial patterns, we identify

310 some common traits. A dominant pattern of precipitation decrease is localized to the Westernmost part of Czechia during winter and expands to the rest of the country during spring. Evapotranspiration increases of the highest magnitude take place during spring and summer. As a result of this opposing direction, during spring, we see the most substantial decrease in runoff and $P - E$ therein. Furthermore, it is safe to state that if evapotranspiration generally increases despite decreasing patches of precipitation (present to a greater or lesser extent across all seasons), the water cycle in Czechia is dominated by changes in

315 energy rather than water availability.

TerraClimate, with a resolution of 4 km, offers far more detail on spatial patterns than other data sets (Figure 8). It has a semester split for precipitation, with a decreasing pattern dominating winter and spring and an increasing pattern dominating summer and autumn. Evapotranspiration decreases during spring and summer but does not cover nearly as much area of Czechia as precipitation when decreasing. Runoff changes circumscribe winter (increase) and spring (decrease) and are rel-

320 atively mute during summer and autumn. Regarding water availability, the patterns of $P - E$ reflect those of precipitation. However, the increases in summer and autumn are not as notable. Autumn is a season of spatial homogeneity in TerraClimate because precipitation, evapotranspiration, runoff, and $P - E$ all depict countrywide increases, albeit of smaller magnitude than in other seasons. On the other hand, a distinctive contrast takes place in winter, in which we have a decrease in runoff in spite of an increase in water availability.

325 Seasonal spatial patterns of mHM have the least substantial changes, with magnitudes mainly in the -25 mm to 25 mm range compared to the -40 mm to 40 mm range of TerraClimate and ERA5-Land (Figure S3). Precipitation patterns mimic those of TerraClimate except for autumn, where mHM(E-OBS) holds more heterogeneity. Contemporaneously, we observe slightly decreased evapotranspiration. For the rest of the seasons, evapotranspiration presents a widespread pattern of positive changes, with the highest magnitudes in summer. There is a dominant decreasing pattern for runoff across all seasons. In winter, there are

330 pinpoint increases around the Czech borders near the Sudetic, Šumava, and Ore Mountains. $P - E$ has the highest magnitude for decreasing change in spring. There is a mixed pattern of increase and decrease for $P - E$ in winter and summer, yet the extent of decreasing changes is more prominent. Once again, analogous to TerraClimate, we find a season of contrasting runoff (decreasing) and $P - E$ (increasing) changes, but for mHM, it takes place in autumn.

mHM spatial pattern of changes in seasonal median water fluxes over Czechia between two 30-year periods: 1961-1990 and

335 1991-2020. I.e., the value of each grid cell is equal to the seasonal median value of 1991-2020 minus the seasonal median value of 1961-1990. P is precipitation, E is evapotranspiration, Q is runoff, and $P - E$ is precipitation minus evapotranspiration. The seasons are defined as follows: winter as December, January, and February; spring as March, April, and May; summer as June, July, and August; autumn as September, October, and November.

ERA5-Land spatial pattern of changes in seasonal median water fluxes closely resembles those of mHM (Figure S4). The

340 previously observed zonal pattern for precipitation change between the two 30-year medians seems to be driven by summer
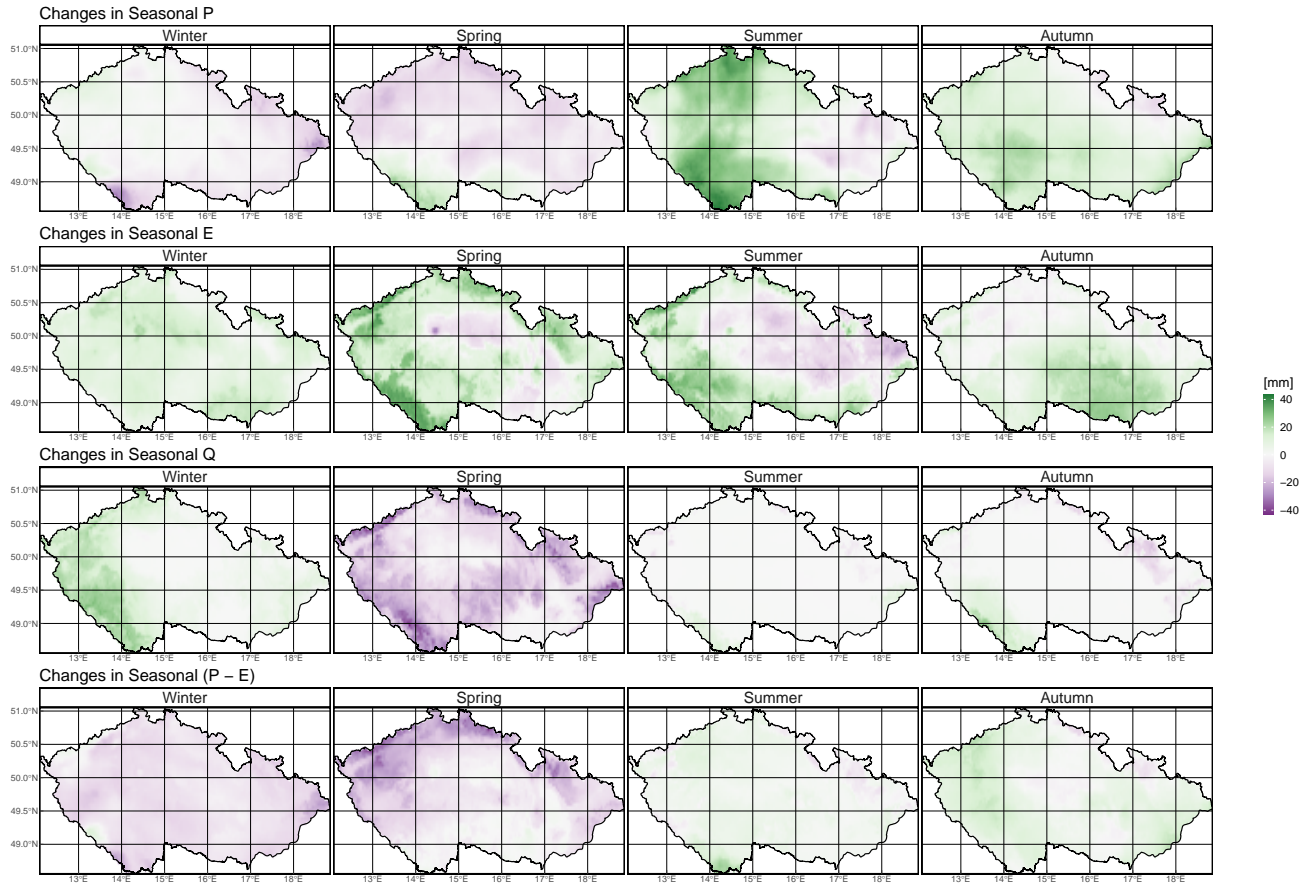
Figure 8. TerraClimate spatial pattern of changes in seasonal median water fluxes over Czechia between two 30-year periods: 1961-1990 and 1991-2020. I.e., the value of each grid cell is equal to the seasonal median value of 1991-2020 minus the seasonal median value of 1961-1990. P is precipitation, E is evapotranspiration, Q is runoff, and $P - E$ is precipitation minus evapotranspiration. The seasons are defined as follows: winter as December, January, and February; spring as March, April, and May; summer as June, July, and August; autumn as September, October, and November.

changes. Evapotranspiration changes, unlike TerraClimate or mHM, are increasing across all seasons. With specifically large evapotranspiration increases in summer followed by spring. In opposition, runoff has decreased regardless of the season. The sporadic patches of increased runoff observed in mHM near the Czech borders are nonexistent in ERA5-Land. Similarly, the mixed patterns for $P - E$ for mHM present in winter and summer are missing in ERA5-Land, which only reports decreasing

345 changes. Lastly, we evince contrast in the direction of change between runoff (predominantly decreasing) and $P - E$ (predominantly increasing) in autumn, parallel to that of mHM. While this contrast is present in all data sets, the season differs for mHM and ERA5-Land (autumn) vs. TerraClimate (winter). Moreover, it is also inversed, i.e., TerraClimate has increasing runoff and decreasing $P - E$, but mHM and ERA5-Land have decreasing runoff and increasing $P - E$.

~~ERA5-Land spatial pattern of changes in seasonal median water fluxes over Czechia between two 30-year periods: 1961-1990~~
350 ~~and 1991-2020. I.e., the value of each grid cell is equal to the seasonal median value of 1991-2020 minus the seasonal median~~
~~value of 1961-1990. P is precipitation, E is evapotranspiration, Q is runoff, and $P - E$ is precipitation minus evapotranspiration.~~
~~The seasons are defined as follows: winter as December, January, and February; spring as March, April, and May; summer as~~
~~June, July, and August; autumn as September, October, and November.~~

4 Discussion

355 Overall long-term changes in the annual water cycle in Czechia are primarily evident in evapotranspiration. Interestingly, the general agreement among different data sets at low-frequency time scales dissolves as we deepen into seasonal and monthly scales. Higher frequency temporal analysis revealed that while its seasonality modulates changes in precipitation, these changes are overwhelmed by a consistent evapotranspiration increase. This compound behavior results in depleted water availability, as reflected by decreasing runoff and $P - E$. Furthermore, different data combinations estimate different spatiotemporal patterns
360 of water cycle changes. The observed redistribution of water availability can seriously impact water resources in the region, including the quality and quantity of drinking water, the accessibility of water for irrigation and energy generation, and the health of aquatic ecosystems. Our results herein provide an updated overview of the water cycle in Czechia and map changes in the past 60 years, are essential to assess and ensure the sustainable use and management of water resources in Czechia. Additionally, we have defined and demonstrated the ability of a purely empirical ranking method to benchmark hydroclimatic
365 data fusion and determine the best combination to represent water cycle budget closure that can be applied to any other regional study.

We determined that the best data sets for long-term assessment of water cycle individual components in Czechia based on the selected references are: mHM(E-OBS), ERA5-Land, and TerraClimate for precipitation; ERA5-Land, mHM, and TerraClimate for evapotranspiration; mHM, TerraClimate, and ERA5-Land for runoff. Similar standings for precipitation data were reported
370 by Fallah et al. (2020) and Bandhauer et al. (2022). Fallah et al. (2020) used runoff simulation vs. streamflow observations using different data sets to benchmark precipitation data and found that E-OBS yields a robust agreement, while ERA5, Global Precipitation Climatology Centre (GPCC V.2018; Schneider et al., 2011), and Multi-Source Weighted-Ensemble Precipitation (MSWEP V2; Beck et al., 2019) show good performances. Bandhauer et al. (2022) report that while E-OBS and ERA5 agree

qualitatively, ERA5 considerably overestimates mean precipitation over Europe due to too many wet days. These prevalent wet bias in ERA5 has been reported along diverse assessments (e.g., Bešt´áková et al., 2022; Lavers et al., 2022). NCEP/NCAR R1 had the worst precipitation performance. It was previously reported that, at least regarding extreme precipitation, NCEP/NCAR R1 performed far better than ERA5's predecessors, i.e., ERA40 (Uppala et al., 2005) and ERA-Interim (Dee et al., 2011), (Sun et al., 2018). This disagreement could be attributed to the improvements implemented in ERA5 over its predecessors in model parameterizations, spatial resolution, and input data assimilation. Additionally, the poor performance of NCEP/NCAR R1 might be rooted in its coarse spatial resolution (two grid cells cover Czechia).

Regarding evapotranspiration estimates, ERA5-Land has been reported as an adequate data source to overcome the unavailability of observed agrometeorological data in Europe (Vanella et al., 2022), and its robustness supports its use for drought monitoring (Vicente-Serrano et al., 2022). mHM has undergone extensive evaluation over Europe at multiple spatial scales and has repeatedly shown its ability to capture the observed dynamics of actual evapotranspiration (Hanel et al., 2018; Rakovec et al., 2016a) and its application to determine dominant drought types and their evolution (Markonis et al., 2021). While, to our knowledge, there have not been studies focusing on the quality or applications of TerraClimate evapotranspiration to date, it has been calibrated and validated using FLUXNET data (Abatzoglou et al., 2018), a conglomerate of networks gathering and standardizing quality control protocols for station-based evapotranspiration measurements (Pastorello et al., 2020). Most of the abovementioned referenced studies also testify to the quality of runoff data from mHM, TerraClimate, and ERA5-Land because the studies use runoff and streamflow data derived, among other variables, from their evapotranspiration estimates and show that they can capture the streamflow dynamics adequately across a wide range of climate and physiographical characteristics.

~~Despite our~~ Our evaluation of individual water cycle components ~~being~~ is cohesive with previous literature~~and~~. Although the data products assessed herein have been previously analyzed at multiple spatial scales, this is done under a univariate perspective, that does not consider the ability of the data sets to reproduce the water cycle and its changes as a whole in a structurally plausible manner. This is easily denoted by the fact that even though mHM's performance was ~~among~~ the best for all water cycle components evaluated using high-quality observational references, the best data set combination ranking is actually ~~Terraclimate~~ TerraClimate exclusive (i.e., all flux estimates from the same data set). ~~Further,~~ Note that the score metric and ranking framework proposed herein serve as a method that can easily and quickly filter out the data set combinations providing implausible results. It should be remarked that this ranking framework acts as an initial assessment to be complemented with additional analyses because the score metric does not account for any biases in the products. Expressly because the aim of our work is not to benchmark the different data sets analyzed herein but to demonstrate how different can become the water cycles depicted by each of them.

It is clear that the story to be told in terms of water cycle changes is not only dependant on the data set of choice but also on the time scale. This kind of differences tend to be overlook when annual averages are being compared but when it comes to annual totals the small discrepancies add up. By further digging into this we unveiled some substantial inconsistency in the ERA5-Land data. It appears that the cumulative sum of the water budget residual in ERA5-Land declines monotonically in time, implying some systematic bias in the water budget closure. Notwithstanding, to our surprise, we found that throughout our analysis, mHM and ERA5-Land (a hydrological model and reanalysis~~(mHM and ERA5-Land)~~ presented more compat-

ible spatiotemporal patterns than the two hydrological models (mHM and TerraClimate). Regarding hydrological models, their evapotranspiration response is strongly linked to how they represent soil moisture and radiative energy at the surface (Boé and Terray, 2008; Zhao et al., 2013), leading to the visible discrepancies among mHM and TerraClimate. In terms of water cycle fluxes' magnitude, we report significant ERA5-Land overestimation of precipitation and evapotranspiration, which are in line with previously reported overestimations of summer precipitation over Central Europe (Hassler and Lauer, 2021; Rivoire et al., 2022). ~~Regarding hydrological models, their evapotranspiration response is strongly linked to how they represent soil moisture and radiative energy at the surface (Boé and Terray, 2008; Zhao et al., 2013), leading to the visible discrepancies among mHM and TerraClimate.~~ These biases in conjunction with the monotonic declining trend we found in the cumulative sum of water budget residual raise further questions about the applicability of ERA5-Land in hydrological studies. Therefore extra caution should be exercised when the widely-used reanalysis data product is employed.

There is agreement among the best-ranked data set combinations that most of the significant changes in Czech water fluxes are localized in spring, particularly in April and May. Notwithstanding, we observe that it is the summer season whose changes determine the spatiotemporal patterns of change between the 1991-2020 and 1961-1990 medians. Declining precipitation and increasing evapotranspiration in spring support reported drying trends over Czechia (Brázdil et al., 2015). In addition to these general patterns, we identified localized increases in winter runoff coupled with decreases and shifts in spring runoff around the Sudetic, Šumava, and Ore Mountains. These changes in mountainous runoff have been previously identified and attributed to decreasing snow cover and earlier snowmelt season (Nedelcev and Jenicek, 2021), which in some Czech catchments also derive in summer low flows (Jenicek and Ledvinka, 2020). Similar seasonal developments of the snow effect on runoff have been reported over multiple mountainous catchments across the world (Berghuijs et al., 2014; Dierauer et al., 2018; Muelchi et al., 2021). Hänsel et al. (2019) remark that seasonal trends are sensitive to shifts in the season definition by one month, which aligns with our monthly analysis because we identified significant changes in months like May and November (peripheral months of spring and autumn as defined herein). Additionally, it could be the reason behind summer, the contiguous season, dominating the long-term precipitation pattern.

The drying regime we report in Czechia, due to the gradual increase in atmospheric evaporative demand over the last 60 years (1961-2020) extends in time and space over central and eastern Europe (Bešt´áková et al., 2022). Jaagus et al. (2022) reported long-term drying trends for the 1949-2018 period in Slovakia, Hungary, Romania, Moldova, southern Poland, and particularly significant in Czechia. Trnka et al. (2016) described a strong tendency towards increased dryness in most Central Europe. Brázdil et al. (2009) performed one of the longest-record analysis in the region (1881-2006) and exposed an increasing tendency towards more prolonged and more intensive dry episodes. Still, it remains unclear how this long-term shift is linked to the post-2000 seasonal (Potopová et al., 2015), annual (Hanel et al., 2018), and multi-year droughts (Moravec et al., 2021) that have occurred in Central Europe and Czechia in specific. It has been demonstrated, though, that these droughts manifest more as soil moisture deficits than meteorological and hydrological droughts, as they are related to high evaporative demand during the warm season period (Markonis et al., 2021). Our results agreement shows that the long-term aridification could be the outcome of the same physical mechanism, i.e., evaporation increase, to the one that dominates the short-term extreme events.

Our study comes with certain limitations that pave the way for future research. A certain limitation is that our analyses do not attribute the observed changes to any potential physical or anthropogenic drivers. It is likely that the evapotranspiration increase is linked to long-term changes in atmospheric circulation patterns that have caused a decline in cloudiness (Lhotka et al., 2020). As it has been shown that global warming is going to disrupt the terrestrial water cycle mainly due to changes in precipitation (Roderick et al., 2014), it is more plausible to attribute the observed intensification to the fluctuations of atmospheric circulation. Yet, this remains to be confirmed by future studies that will determine the factors that contribute most to the hydroclimatic shifts, although drought projections over Czechia (Dubrovsky et al., 2009), and central Europe Hari et al. (2020) indicate an increased drought risk in the future prevalent under different climate change scenarios. Additionally, our work does not investigate the role of water storage (snow and groundwater), as well as land cover or vegetation changes. Lastly, while country-level assessments are essential to improve water resources management and natural hazard policies, the water cycle budget is closed over hydrological units, not administrative boundaries.

5   Conclusions

Herein, we have proposed and demonstrated the applicability of a novel benchmarking method based on water cycle budget closure for hydroclimatic data fusion. The method does not enforce closure nor merge multiple data sets into a new one, but instead identifies the best combination of data sets in terms of water cycle budget residual distribution and correlation to referential data. Furthermore, the ranking method presented could easily be applied to any other region and use different referential data sets for evaluation. The ranking method may still be employed using gridded data like GPCC or CRU TS as an evaluation reference in data-scarce areas or when ground-station data is not publicly available. Most importantly, this metric is not constrained by data availability, as any of the variables in the equation evaluation terms can be omitted. This modularity makes it a flexible alternative to traditional approaches.

Using the best water budget data, we demonstrate that Czechia is undergoing water cycle acceleration, evinced by increased atmospheric water demand. Remarkably, the increase in precipitation is not as pronounced as that one in evapotranspiration. While changes in the 30-year median of spatial weight average annual values show a minimum change in water availability, the spatial patterns reveal a prevalent decreasing pattern of runoff across the country. Besides, we identified significant spatial heterogeneity when assessing precipitation at a seasonal scale. Intriguingly, summer patterns are reflected in the spatial difference between the 1991-2020 and the 1961-1990 medians despite most of the significant changes in water cycle components being localized in spring. What is more, the precipitation rain/snow partition effect of less snow and earlier snowmelt around the mountains is reflected in a seasonal shift of runoff (increase in winter and subsequent decrease in spring). This might reflect how sub-seasonal shifts could affect the long-term hydrologic changes.

Based on our results and previous literature, it is safe to state that the depletion of water availability (runoff and $P - E$) over Czechia could prompt a surge in drought frequency. Considering that shifts in evapotranspiration overwhelm those of precipitation, the water cycle in Czechia is mainly driven by changes in energy rather than water availability. Further research is needed to better understand the complex drivers of this drying trend and to develop targeted interventions to address possible

factors external to natural variability, like land-use changes and other anthropogenic factors. Although it remains unknown if this drying trend will persist, it should be considered in the planning of effective drought management strategies and water conservation measures to mitigate its adverse impacts for agriculture, energy production, and natural ecosystems in Czechia.

References

Abatzoglou, J. T., Dobrowski, S. Z., Parks, S. A., and Hegewisch, K. C.: TerraClimate, a high-resolution global dataset of monthly climate and climatic water balance from 1958–2015, Scientific Data, 5, 170 191, https://doi.org/10.1038/sdata.2017.191, number: 1 Publisher: Nature Publishing Group, 2018.

Aires, F.: Combining datasets of satellite-retrieved products. Part I: Methodology and water budget closure, Journal of Hydrometeorology, 15, 1677–1691, 2014.

Allan, R. P.: Regime dependent changes in global precipitation, Climate Dynamics, 39, 827–840, 2012.

Bai, P. and Liu, X.: Intercomparison and evaluation of three global high-resolution evapotranspiration products across China, Journal of Hydrology, 566, 743–755, https://doi.org/10.1016/j.jhydrol.2018.09.065, 2018.

Bandhauer, M., Isotta, F., Lakatos, M., Lussana, C., Båserud, L., Izsák, B., Szentes, O., Tveito, O. E., and Frei, C.: Evaluation of daily precipitation analyses in E-OBS (v19.0e) and ERA5 by comparison to regional high-resolution datasets in European regions, International Journal of Climatology, 42, 727–747, https://doi.org/10.1002/joc.7269, _eprint: https://onlinelibrary.wiley.com/doi/pdf/10.1002/joc.7269, 2022.

Beck, H. E., Pan, M., Roy, T., Weedon, G. P., Pappenberger, F., van Dijk, A. I. J. M., Huffman, G. J., Adler, R. F., and Wood, E. F.: Daily evaluation of 26 precipitation datasets using Stage-IV gauge-radar data for the CONUS, Hydrology and Earth System Sciences, 23, 207–224, https://doi.org/10.5194/hess-23-207-2019, publisher: Copernicus GmbH, 2019.

Berghuijs, W. R., Woods, R. A., and Hrachowitz, M.: A precipitation shift from snow towards rain leads to a decrease in streamflow, Nature Climate Change, 4, 583–586, https://doi.org/10.1038/nclimate2246, number: 7 Publisher: Nature Publishing Group, 2014.

Bešťáková, Z., Strnad, F., Vargas Godoy, M. R., Singh, U., Markonis, Y., Hanel, M., Máca, P., and Kyselý, J.: Changes of the aridity index in Europe from 1950 to 2019, Theoretical and Applied Climatology, https://doi.org/10.1007/s00704-022-04266-3, 2022.

Boé, J. and Terray, L.: Uncertainties in summer evapotranspiration changes over Europe and implications for regional climate change, Geophysical Research Letters, 35, https://doi.org/10.1029/2007GL032417, _eprint: https://onlinelibrary.wiley.com/doi/pdf/10.1029/2007GL032417, 2008.

Brázdil, R., Trnka, M., Dobrovolný, P., Chromá, K., Hlavinka, P., and Žalud, Z.: Variability of droughts in the Czech Republic, 1881–2006, Theoretical and Applied Climatology, 97, 297–315, https://doi.org/10.1007/s00704-008-0065-x, 2009.

Brázdil, R., Dobrovolný, P., Trnka, M., Kotyza, O., Řezníčková, L., Valášek, H., Zahradníček, P., and Štěpánek, P.: Droughts in the Czech Lands, 1090–2012 AD, Climate of the Past, 9, 1985–2002, https://doi.org/10.5194/cp-9-1985-2013, publisher: Copernicus GmbH, 2013.

Brázdil, R., Trnka, M., Mikšovský, J., Řezníčková, L., and Dobrovolný, P.: Spring-summer droughts in the Czech Land in 1805–2012 and their forcings, International Journal of Climatology, 35, 1405–1421, https://doi.org/10.1002/joc.4065, _eprint: https://onlinelibrary.wiley.com/doi/pdf/10.1002/joc.4065, 2015.

Chen, M., Xie, P., Janowiak, J. E., and Arkin, P. A.: Global land precipitation: A 50-yr monthly analysis based on gauge observations, Journal of Hydrometeorology, 3, 249–266, 2002.

Cornes, R. C., van der Schrier, G., van den Besselaar, E. J. M., and Jones, P. D.: An Ensemble Version of the E-OBS Temperature and Precipitation Data Sets, Journal of Geophysical Research: Atmospheres, 123, 9391–9409, https://doi.org/10.1029/2017JD028200, _eprint: https://onlinelibrary.wiley.com/doi/pdf/10.1029/2017JD028200, 2018.

Dee, D. P., Uppala, S. M., Simmons, A. J., Berrisford, P., Poli, P., Kobayashi, S., Andrae, U., Balmaseda, M. A., Balsamo, G., and Bauer, d. P.: The ERA-Interim reanalysis: Configuration and performance of the data assimilation system, Quarterly Journal of the royal meteorological society, 137, 553–597, 2011.

530 Dierauer, J. R., Whitfield, P. H., and Allen, D. M.: Climate Controls on Runoff and Low Flows in Mountain Catchments of Western North America, Water Resources Research, 54, 7495–7510, https://doi.org/10.1029/2018WR023087, _eprint: https://onlinelibrary.wiley.com/doi/pdf/10.1029/2018WR023087, 2018.

Dubrovsky, M., Svoboda, M. D., Trnka, M., Hayes, M. J., Wilhite, D. A., Zalud, Z., and Hlavinka, P.: Application of relative drought indices in assessing climate-change impacts on drought conditions in Czechia, Theoretical and Applied Climatology, 96, 155–171,
535 https://doi.org/10.1007/s00704-008-0020-x, 2009.

Fallah, A., O, S., and Orth, R.: Climate-dependent propagation of precipitation uncertainty into the water cycle, Hydrology and Earth System Sciences, 24, 3725–3735, https://doi.org/10.5194/hess-24-3725-2020, publisher: Copernicus GmbH, 2020.

Fick, S. E. and Hijmans, R. J.: WorldClim 2: new 1-km spatial resolution climate surfaces for global land areas, International Journal of Climatology, 37, 4302–4315, https://doi.org/10.1002/joc.5086, _eprint: https://onlinelibrary.wiley.com/doi/pdf/10.1002/joc.5086, 2017.

540 Ghiggi, G., Humphrey, V., Seneviratne, S. I., and Gudmundsson, L.: GRUN: an observation-based global gridded runoff dataset from 1902 to 2014, Earth System Science Data, 11, 1655–1674, publisher: Copernicus, 2019.

Hanel, M., Rakovec, O., Markonis, Y., Máca, P., Samaniego, L., Kyselý, J., and Kumar, R.: Revisiting the recent European droughts from a long-term perspective, Scientific Reports, 8, 9499, https://doi.org/10.1038/s41598-018-27464-4, number: 1 Publisher: Nature Publishing Group, 2018.

545 Hargreaves, G. H. and Samani, Z. A.: Estimating Potential Evapotranspiration, Journal of the Irrigation and Drainage Division, 108, 225–230, https://doi.org/10.1061/JRCEA4.0001390, publisher: American Society of Civil Engineers, 1982.

Hari, V., Rakovec, O., Markonis, Y., Hanel, M., and Kumar, R.: Increased future occurrences of the exceptional 2018–2019 Central European drought under global warming, Scientific Reports, 10, 12 207, https://doi.org/10.1038/s41598-020-68872-9, number: 1 Publisher: Nature Publishing Group, 2020.

550 Harris, I., Osborn, T. J., Jones, P., and Lister, D.: Version 4 of the CRU TS monthly high-resolution gridded multivariate climate dataset, Scientific data, 7, 1–18, publisher: Nature Publishing Group, 2020.

Hassler, B. and Lauer, A.: Comparison of Reanalysis and Observational Precipitation Datasets Including ERA5 and WFDE5, Atmosphere, 12, 1462, https://doi.org/10.3390/atmos12111462, number: 11 Publisher: Multidisciplinary Digital Publishing Institute, 2021.

Held, I. M. and Soden, B. J.: Robust Responses of the Hydrological Cycle to Global Warming, Journal of Climate, 19, 5686–5699,
555 https://doi.org/10.1175/JCLI3990.1, publisher: American Meteorological Society Section: Journal of Climate, 2006.

Hijmans, R. J., Cameron, S. E., Parra, J. L., Jones, P. G., and Jarvis, A.: Very high resolution interpolated climate surfaces for global land areas, International Journal of Climatology, 25, 1965–1978, https://doi.org/10.1002/joc.1276, _eprint: https://onlinelibrary.wiley.com/doi/pdf/10.1002/joc.1276, 2005.

Hu, Y., Duan, W., Chen, Y., Zou, S., Kayumba, P. M., and Sahu, N.: An integrated assessment of runoff dynamics in the Amu
560 Darya River Basin: Confronting climate change and multiple human activities, 1960–2017, Journal of Hydrology, 603, 126 905, https://doi.org/10.1016/j.jhydrol.2021.126905, 2021.

Hänsel, S., Ustrnul, Z., Łupikasza, E., and Skalak, P.: Assessing seasonal drought variations and trends over Central Europe, Advances in Water Resources, 127, 53–75, https://doi.org/10.1016/j.advwatres.2019.03.005, 2019.

Jaagus, J., Aasa, A., Aniskevich, S., Boincean, B., Bojariu, R., Briede, A., Danilovich, I., Castro, F. D., Dumitrescu, A., Labuda, M., Labudová, L., Lõhmus, K., Melnik, V., Mõisja, K., Pongracz, R., Potopová, V., Řezníčková, L., Rimkus, E., Semenova, I., Stonevičius, E., Štěpánek, P., Trnka, M., Vicente-Serrano, S. M., Wibig, J., and Zahradníček, P.: Long-term changes in drought indices in eastern and central Europe, International Journal of Climatology, 42, 225–249, https://doi.org/10.1002/joc.7241, _eprint: https://onlinelibrary.wiley.com/doi/pdf/10.1002/joc.7241, 2022.

Janowiak, J. E. and Xie, P.: CAMS–OPI: A Global Satellite–Rain Gauge Merged Product for Real-Time Precipitation Monitoring Applications, Journal of Climate, 12, 3335–3342, https://doi.org/10.1175/1520-0442(1999)012<3335:COAGSR>2.0.CO;2, publisher: American Meteorological Society Section: Journal of Climate, 1999.

Jenicek, M. and Ledvinka, O.: Importance of snowmelt contribution to seasonal runoff and summer low flows in Czechia, Hydrology and Earth System Sciences, 24, 3475–3491, https://doi.org/10.5194/hess-24-3475-2020, publisher: Copernicus GmbH, 2020.

Jenicek, M., Hnilica, J., Nedelcev, O., and Sipek, V.: Future changes in snowpack will impact seasonal runoff and low flows in Czechia, Journal of Hydrology: Regional Studies, 37, 100 899, https://doi.org/10.1016/j.ejrh.2021.100899, 2021.

Kalnay, E., Kanamitsu, M., Kistler, R., Collins, W., Deaven, D., Gandin, L., Iredell, M., Saha, S., White, G., and Woollen, J.: The NCEP/NCAR 40-year reanalysis project, Bulletin of the American meteorological Society, 77, 437–472, 1996.

Kašpar, M., Bližňák, V., Hulec, F., and Müller, M.: High-resolution spatial analysis of the variability in the subdaily rainfall time structure, Atmospheric Research, 248, 105 202, https://doi.org/10.1016/j.atmosres.2020.105202, 2021.

Kašpárek, L. and Kožín, R.: Changes in precipitation and runoff in river basins in the Czech Republic during the period of intense warming, Vodohospodářské technicko-ekonomické informace, 64, 12–27, publisher: Výzkumný ústav vodohospodářský T. G. Masaryka, veřejná výzkumná instituce, 2022.

Kobayashi, S., Ota, Y., Harada, Y., Ebita, A., Moriya, M., Onoda, H., Onogi, K., Kamahori, H., Kobayashi, C., Endo, H., Miyaoka, K., and Takahashi, K.: The JRA-55 Reanalysis: General Specifications and Basic Characteristics, Journal of the Meteorological Society of Japan. Ser. II, 93, 5–48, https://doi.org/10.2151/jmsj.2015-001, 2015.

Kumar, R., Samaniego, L., and Attinger, S.: Implications of distributed hydrologic model parameterization on water fluxes at multiple scales and locations, Water Resources Research, 49, 360–379, https://doi.org/10.1029/2012WR012195, _eprint: https://onlinelibrary.wiley.com/doi/pdf/10.1029/2012WR012195, 2013.

Kyselý, J. and Beranová, R.: Climate-change effects on extreme precipitation in central Europe: uncertainties of scenarios based on regional climate models, Theoretical and Applied Climatology, 95, 361–374, https://doi.org/10.1007/s00704-008-0014-8, 2009.

Kyselý, J., Gaál, L., Beranová, R., and Plavcová, E.: Climate change scenarios of precipitation extremes in Central Europe from ENSEMBLES regional climate models, Theoretical and Applied Climatology, 104, 529–542, https://doi.org/10.1007/s00704-010-0362-z, 2011.

Lavers, D. A., Simmons, A., Vamborg, F., and Rodwell, M. J.: An evaluation of ERA5 precipitation for climate monitoring, Quarterly Journal of the Royal Meteorological Society, 148, 3152–3165, https://doi.org/10.1002/qj.4351, _eprint: https://onlinelibrary.wiley.com/doi/pdf/10.1002/qj.4351, 2022.

Lhotka, O., Trnka, M., Kyselý, J., Markonis, Y., Balek, J., and Možný, M.: Atmospheric Circulation as a Factor Contributing to Increasing Drought Severity in Central Europe, Journal of Geophysical Research: Atmospheres, 125, e2019JD032 269, https://doi.org/10.1029/2019JD032269, _eprint: https://onlinelibrary.wiley.com/doi/pdf/10.1029/2019JD032269, 2020.

Liu, J., Zhang, J., Kong, D., Feng, X., Feng, S., and Xiao, M.: Contributions of Anthropogenic Forcings to Evapotranspiration Changes Over 1980–2020 Using GLEAM and CMIP6 Simulations, Journal of Geophysical Research: Atmospheres, 126, e2021JD035 367, https://doi.org/10.1029/2021JD035367, _eprint: https://onlinelibrary.wiley.com/doi/pdf/10.1029/2021JD035367, 2021.

Lorenz, C. and Kunstmann, H.: The Hydrological Cycle in Three State-of-the-Art Reanalyses: Intercomparison and Performance Analysis, Journal of Hydrometeorology, 13, 1397–1420, https://doi.org/10.1175/JHM-D-11-088.1, publisher: American Meteorological Society Section: Journal of Hydrometeorology, 2012.

Markonis, Y., Kumar, R., Hanel, M., Rakovec, O., Máca, P., and AghaKouchak, A.: The rise of compound warm-season droughts in Europe, Science Advances, 7, eabb9668, https://doi.org/10.1126/sciadv.abb9668, publisher: American Association for the Advancement of Science, 2021.

Martens, B., Gonzalez Miralles, D., Lievens, H., Van Der Schalie, R., De Jeu, R. A., Fernández-Prieto, D., Beck, H. E., Dorigo, W., and Verhoest, N.: GLEAM v3: Satellite-based land evaporation and root-zone soil moisture, Geoscientific Model Development, 10, 1903–1925, 2017.

Mei, Y., Mai, J., Do, H. X., Gronewold, A., Reeves, H., Eberts, S., Niswonger, R., Regan, R. S., and Hunt, R. J.: Can Hydrological Models Benefit From Using Global Soil Moisture, Evapotranspiration, and Runoff Products as Calibration Targets?, Water Resources Research, 59, e2022WR032 064, https://doi.org/10.1029/2022WR032064, _eprint: https://onlinelibrary.wiley.com/doi/pdf/10.1029/2022WR032064, 2023.

Moazamnia, M., Hassanzadeh, Y., Nadiri, A. A., Khatibi, R., and Sadeghfam, S.: Formulating a strategy to combine artificial intelligence models using Bayesian model averaging to study a distressed aquifer with sparse data availability, Journal of Hydrology, 571, 765–781, https://doi.org/10.1016/j.jhydrol.2019.02.011, 2019.

Moravec, V., Markonis, Y., Rakovec, O., Svoboda, M., Trnka, M., Kumar, R., and Hanel, M.: Europe under multi-year droughts: how severe was the 2014–2018 drought period?, Environmental Research Letters, 16, 034 062, https://doi.org/10.1088/1748-9326/abe828, publisher: IOP Publishing, 2021.

Mozny, M., Trnka, M., Vlach, V., Vizina, A., Potopova, V., Zahradnicek, P., Stepanek, P., Hajkova, L., Staponites, L., and Zalud, Z.: Past (1971–2018) and future (2021–2100) pan evaporation rates in the Czech Republic, Journal of Hydrology, 590, 125 390, https://doi.org/10.1016/j.jhydrol.2020.125390, 2020.

Muelchi, R., Rössler, O., Schwanbeck, J., Weingartner, R., and Martius, O.: River runoff in Switzerland in a changing climate – runoff regime changes and their time of emergence, Hydrology and Earth System Sciences, 25, 3071–3086, https://doi.org/10.5194/hess-25-3071-2021, publisher: Copernicus GmbH, 2021.

Munier, S. and Aires, F.: A new global method of satellite dataset merging and quality characterization constrained by the terrestrial water budget, Remote Sensing of Environment, 205, 119–130, publisher: Elsevier, 2018.

Muñoz-Sabater, J., Dutra, E., Agustí-Panareda, A., Albergel, C., Arduini, G., Balsamo, G., Boussetta, S., Choulga, M., Harrigan, S., Hersbach, H., Martens, B., Miralles, D. G., Piles, M., Rodríguez-Fernández, N. J., Zsoter, E., Buontempo, C., and Thépaut, J.-N.: ERA5-Land: a state-of-the-art global reanalysis dataset for land applications, Earth System Science Data, 13, 4349–4383, https://doi.org/10.5194/essd-13-4349-2021, publisher: Copernicus GmbH, 2021.

Nedelcev, O. and Jenicek, M.: Trends in seasonal snowpack and their relation to climate variables in mountain catchments in Czechia, Hydrological Sciences Journal, 66, 2340–2356, https://doi.org/10.1080/02626667.2021.1990298, publisher: Taylor & Francis _eprint: https://doi.org/10.1080/02626667.2021.1990298, 2021.

Pan, M. and Wood, E. F.: Data assimilation for estimating the terrestrial water budget using a constrained ensemble Kalman filter, Journal of Hydrometeorology, 7, 534–547, 2006.

Pan, M., Sahoo, A. K., Troy, T. J., Vinukollu, R. K., Sheffield, J., and Wood, E. F.: Multisource estimation of long-term terrestrial water budget for major global river basins, Journal of Climate, 25, 3191–3206, 2012.

640 Pastorello, G., Trotta, C., Canfora, E., Chu, H., Christianson, D., Cheah, Y.-W., Poindexter, C., Chen, J., Elbashandy, A., Humphrey, M., Isaac, P., Polidori, D., Reichstein, M., Ribeca, A., van Ingen, C., Vuichard, N., Zhang, L., Amiro, B., Ammann, C., Arain, M. A., Ardö, J., Arkebauer, T., Arndt, S. K., Arriga, N., Aubinet, M., Aurela, M., Baldocchi, D., Barr, A., Beamesderfer, E., Marchesini, L. B., Bergeron, O., Beringer, J., Bernhofer, C., Berveiller, D., Billesbach, D., Black, T. A., Blanken, P. D., Bohrer, G., Boike, J., Bolstad, P. V., Bonal, D., Bonnefond, J.-M., Bowling, D. R., Bracho, R., Brodeur, J., Brümmer, C., Buchmann, N., Burban, B., Burns, S. P., Buysse, P., Cale, P.,

645 Cavagna, M., Cellier, P., Chen, S., Chini, I., Christensen, T. R., Cleverly, J., Collalti, A., Consalvo, C., Cook, B. D., Cook, D., Coursolle, C., Cremonese, E., Curtis, P. S., D'Andrea, E., da Rocha, H., Dai, X., Davis, K. J., Cinti, B. D., Grandcourt, A. d., Ligne, A. D., De Oliveira, R. C., Delpierre, N., Desai, A. R., Di Bella, C. M., Tommasi, P. d., Dolman, H., Domingo, F., Dong, G., Dore, S., Duce, P., Dufrêne, E., Dunn, A., Dušek, J., Eamus, D., Eichelmann, U., ElKhidir, H. A. M., Eugster, W., Ewenz, C. M., Ewers, B., Famulari, D., Fares, S., Feigenwinter, I., Feitz, A., Fensholt, R., Filippa, G., Fischer, M., Frank, J., Galvagno, M., Gharun, M., Gianelle, D., Gielen, B., Gioli, B.,

650 Gitelson, A., Goded, I., Goeckede, M., Goldstein, A. H., Gough, C. M., Goulden, M. L., Graf, A., Griebel, A., Gruening, C., Grünwald, T., Hammerle, A., Han, S., Han, X., Hansen, B. U., Hanson, C., Hatakka, J., He, Y., Hehn, M., Heinesch, B., Hinko-Najera, N., Hörtnagl, L., Hutley, L., Ibrom, A., Ikawa, H., Jackowicz-Korczynski, M., Janouš, D., Jans, W., Jassal, R., Jiang, S., Kato, T., Khomik, M., Klatt, J., Knohl, A., Knox, S., Kobayashi, H., Koerber, G., Kolle, O., Kosugi, Y., Kotani, A., Kowalski, A., Kruijt, B., Kurbatova, J., Kutsch, W. L., Kwon, H., Launiainen, S., Laurila, T., Law, B., Leuning, R., Li, Y., Liddell, M., Limousin, J.-M., Lion, M., Liska, A. J., Lohila,

655 A., López-Ballesteros, A., López-Blanco, E., Loubet, B., Loustau, D., Lucas-Moffat, A., Lüers, J., Ma, S., Macfarlane, C., Magliulo, V., Maier, R., Mammarella, I., Manca, G., Marcolla, B., Margolis, H. A., Marras, S., Massman, W., Mastepanov, M., Matamala, R., Matthes, J. H., Mazzenga, F., McCaughey, H., McHugh, I., McMillan, A. M. S., Merbold, L., Meyer, W., Meyers, T., Miller, S. D., Minerbi, S., Moderow, U., Monson, R. K., Montagnani, L., Moore, C. E., Moors, E., Moreaux, V., Moureaux, C., Munger, J. W., Nakai, T., Neirynck, J., Nesic, Z., Nicolini, G., Noormets, A., Northwood, M., Nosetto, M., Nouvellon, Y., Novick, K., Oechel, W., Olesen, J. E., Ourcival,

660 J.-M., Papuga, S. A., Parmentier, F.-J., Paul-Limoges, E., Pavelka, M., Peichl, M., Pendall, E., Phillips, R. P., Pilegaard, K., Pirk, N., Posse, G., Powell, T., Prasse, H., Prober, S. M., Rambal, S., Rannik, U., Raz-Yaseef, N., Rebmann, C., Reed, D., Dios, V. R. d., Restrepo-Coupe, N., Reverter, B. R., Roland, M., Sabbatini, S., Sachs, T., Saleska, S. R., Sánchez-Cañete, E. P., Sanchez-Mejia, Z. M., Schmid, H. P., Schmidt, M., Schneider, K., Schrader, F., Schroder, I., Scott, R. L., Sedlák, P., Serrano-Ortíz, P., Shao, C., Shi, P., Shironya, I., Siebicke, L., Šigut, L., Silberstein, R., Sirca, C., Spano, D., Steinbrecher, R., Stevens, R. M., Sturtevant, C., Suyker, A., Tagesson, T.,

665 Takanashi, S., Tang, Y., Tapper, N., Thom, J., Tomassucci, M., Tuovinen, J.-P., Urbanski, S., Valentini, R., van der Molen, M., van Gorsel, E., van Huissteden, K., Varlagin, A., Verfaillie, J., Vesala, T., Vincke, C., Vitale, D., Vygodskaya, N., Walker, J. P., Walter-Shea, E., Wang, H., Weber, R., Westermann, S., Wille, C., Wofsy, S., Wohlfahrt, G., Wolf, S., Woodgate, W., Li, Y., Zampedri, R., Zhang, J., Zhou, G., Zona, D., Agarwal, D., Biraud, S., Torn, M., and Papale, D.: The FLUXNET2015 dataset and the ONEFlux processing pipeline for eddy covariance data, Scientific Data, 7, 225, https://doi.org/10.1038/s41597-020-0534-3, number: 1 Publisher: Nature Publishing Group, 2020.

670 Pellet, V., Aires, F., Munier, S., Fernández Prieto, D., Jordá, G., Dorigo, W. A., Polcher, J., and Brocca, L.: Integrating multiple satellite observations into a coherent dataset to monitor the full water cycle – application to the Mediterranean region, Hydrology and Earth System Sciences, 23, 465–491, https://doi.org/10.5194/hess-23-465-2019, publisher: Copernicus GmbH, 2019.

Peterson, T. C. and Vose, R. S.: An overview of the Global Historical Climatology Network temperature database, Bulletin of the American Meteorological Society, 78, 2837–2850, 1997.

675 Potopová, V., Štěpánek, P., Možný, M., Türkott, L., and Soukup, J.: Performance of the standardised precipitation evapotranspiration index at various lags for agricultural drought risk assessment in the Czech Republic, Agricultural and Forest Meteorology, 202, 26–38, https://doi.org/10.1016/j.agrformet.2014.11.022, 2015.

Povey, A. C. and Grainger, R. G.: Known and unknown unknowns: uncertainty estimation in satellite remote sensing, Atmospheric Measurement Techniques, 8, 4699–4718, https://doi.org/10.5194/amt-8-4699-2015, publisher: Copernicus GmbH, 2015.

680 Priestley, C. H. B. and Taylor, R. J.: On the Assessment of Surface Heat Flux and Evaporation Using Large-Scale Parameters, Monthly Weather Review, 100, 81–92, https://doi.org/10.1175/1520-0493(1972)100<0081:OTAOSH>2.3.CO;2, publisher: American Meteorological Society Section: Monthly Weather Review, 1972.

Rakovec, O., Kumar, R., Attinger, S., and Samaniego, L.: Improving the realism of hydrologic model functioning through multivariate parameter estimation, Water Resources Research, 52, 7779–7792, https://doi.org/10.1002/2016WR019430, _eprint:
685 https://onlinelibrary.wiley.com/doi/pdf/10.1002/2016WR019430, 2016a.

Rakovec, O., Kumar, R., Mai, J., Cuntz, M., Thober, S., Zink, M., Attinger, S., Schäfer, D., Schrön, M., and Samaniego, L.: Multi-scale and Multivariate Evaluation of Water Fluxes and States over European River Basins, Journal of Hydrometeorology, 17, 287–307, https://doi.org/10.1175/JHM-D-15-0054.1, publisher: American Meteorological Society Section: Journal of Hydrometeorology, 2016b.

Rakovec, O., Samaniego, L., Hari, V., Markonis, Y., Moravec, V., Thober, S., Hanel, M., and Kumar, R.: The 2018–2020 Multi-
690 Year Drought Sets a New Benchmark in Europe, Earth's Future, 10, e2021EF002 394, https://doi.org/10.1029/2021EF002394, _eprint: https://onlinelibrary.wiley.com/doi/pdf/10.1029/2021EF002394, 2022.

Rivoire, P., Le Gall, P., Favre, A.-C., Naveau, P., and Martius, O.: High return level estimates of daily ERA-5 precipitation in Europe estimated using regionalized extreme value distributions, Weather and Climate Extremes, 38, 100 500, https://doi.org/10.1016/j.wace.2022.100500, 2022.

695 Rodell, M., Beaudoing, H. K., L'Ecuyer, T., Olson, W. S., Famiglietti, J. S., Houser, P. R., Adler, R., Bosilovich, M. G., Clayson, C. A., Chambers, D., and others: The observed state of the water cycle in the early twenty-first century, Journal of Climate, 28, 8289–8318, 2015.

Roderick, M., Sun, F., Lim, W. H., and Farquhar, G.: A general framework for understanding the response of the water cycle to global warming over land and ocean, Hydrology and Earth System Sciences, 18, 1575–1589, publisher: Copernicus GmbH, 2014.

700 Rodgers, C. D.: Inverse methods for atmospheric sounding: theory and practice, vol. 2, World scientific, 2000.

Sahoo, A. K., Pan, M., Troy, T. J., Vinukollu, R. K., Sheffield, J., and Wood, E. F.: Reconciling the global terrestrial water budget using satellite remote sensing, Remote Sensing of Environment, 115, 1850–1865, publisher: Elsevier, 2011.

Samaniego, L., Kumar, R., and Attinger, S.: Multiscale parameter regionalization of a grid-based hydrologic model at the mesoscale, Water Resources Research, 46, https://doi.org/10.1029/2008WR007327, _eprint:
705 https://onlinelibrary.wiley.com/doi/pdf/10.1029/2008WR007327, 2010.

Samaniego, L., Thober, S., Wanders, N., Pan, M., Rakovec, O., Sheffield, J., Wood, E. F., Prudhomme, C., Rees, G., Houghton-Carr, H., Fry, M., Smith, K., Watts, G., Hisdal, H., Estrela, T., Buontempo, C., Marx, A., and Kumar, R.: Hydrological Forecasts and Projections for Improved Decision-Making in the Water Sector in Europe, Bulletin of the American Meteorological Society, 100, 2451–2472, https://doi.org/10.1175/BAMS-D-17-0274.1, publisher: American Meteorological Society Section: Bulletin of the American Meteorolog-
710 ical Society, 2019.

Schneider, U., Becker, A., Finger, P., Meyer-Christoffer, A., Rudolf, B., and Ziese, M.: GPCC full data reanalysis version 6.0 at 0.5: monthly land-surface precipitation from rain-gauges built on GTS-based and historic data, GPCC Data Rep., doi, 10, 2011.

Schneider, U., Finger, P., Meyer-Christoffer, A., Rustemeier, E., Ziese, M., and Becker, A.: Evaluating the hydrological cycle over land using the newly-corrected precipitation climatology from the Global Precipitation Climatology Centre (GPCC), Atmosphere, 8, 52, 2017.

Sheffield, J., Ferguson, C. R., Troy, T. J., Wood, E. F., and McCabe, M. F.: Closing the terrestrial water budget from satellite remote sensing, Geophysical Research Letters, 36, publisher: Wiley Online Library, 2009.

Skliris, N., Zika, J. D., Nurser, G., Josey, S. A., and Marsh, R.: Global water cycle amplifying at less than the Clausius-Clapeyron rate, Scientific reports, 6, 1–9, publisher: Nature Publishing Group, 2016.

Sun, Q., Miao, C., Duan, Q., Ashouri, H., Sorooshian, S., and Hsu, K.-L.: A review of global precipitation data sets: Data sources, estimation, and intercomparisons, Reviews of Geophysics, 56, 79–107, publisher: Wiley Online Library, 2018.

Svoboda, V., Hanel, M., Máca, P., and Kyselý, J.: Projected changes of rainfall event characteristics for the Czech Republic, Journal of Hydrology and Hydromechanics, 64, 415–425, https://doi.org/10.1515/johh-2016-0036, 2016.

Trenberth, K. E.: Changes in precipitation with climate change, Climate Research, 47, 123–138, 2011.

Trenberth, K. E., Fasullo, J. T., and Mackaro, J.: Atmospheric moisture transports from ocean to land and global energy flows in reanalyses, Journal of Climate, 24, 4907–4924, 2011.

Trnka, M., Balek, J., Štěpánek, P., Zahradníček, P., Možný, M., Eitzinger, J., Žalud, Z., Formayer, H., Turňa, M., Nejedlík, P., Semerádová, D., Hlavinka, P., and Brázdil, R.: Drought trends over part of Central Europe between 1961 and 2014, Climate Research, 70, 143–160, https://doi.org/10.3354/cr01420, 2016.

United Nations: World Population Prospects 2022: Summary of Results, Statistical Papers - United Nations (Ser. A), Population and Vital Statistics Report, United Nations, https://doi.org/10.18356/9789210014380, 2022.

Uppala, S. M., K\aallberg, P., Simmons, A., Andrae, U., Bechtold, V. D. C., Fiorino, M., Gibson, J., Haseler, J., Hernandez, A., Kelly, G., and others: The ERA-40 re-analysis, Quarterly Journal of the Royal Meteorological Society: A journal of the atmospheric sciences, applied meteorology and physical oceanography, 131, 2961–3012, publisher: Wiley Online Library, 2005.

Vanella, D., Longo-Minnolo, G., Belfiore, O. R., Ramírez-Cuesta, J. M., Pappalardo, S., Consoli, S., D'Urso, G., Chirico, G. B., Coppola, A., Comegna, A., Toscano, A., Quarta, R., Provenzano, G., Ippolito, M., Castagna, A., and Gandolfi, C.: Comparing the use of ERA5 reanalysis dataset and ground-based agrometeorological data under different climates and topography in Italy, Journal of Hydrology: Regional Studies, 42, 101 182, https://doi.org/10.1016/j.ejrh.2022.101182, 2022.

Vargas Godoy, M. R., Markonis, Y., Hanel, M., Kyselý, J., and Papalexiou, S. M.: The Global Water Cycle Budget: A Chronological Review, Surveys in Geophysics, 42, 1075–1107, https://doi.org/10.1007/s10712-021-09652-6, 2021.

Vecchi, G. A., Soden, B. J., Wittenberg, A. T., Held, I. M., Leetmaa, A., and Harrison, M. J.: Weakening of tropical Pacific atmospheric circulation due to anthropogenic forcing, Nature, 441, 73, 2006.

Vicente-Serrano, S. M., Domínguez-Castro, F., Reig, F., Tomas-Burguera, M., Peña-Angulo, D., Latorre, B., Beguería, S., Rabanaque, I., Noguera, I., Lorenzo-Lacruz, J., and El Kenawy, A.: A global drought monitoring system and dataset based on ERA5 reanalysis: A focus on crop-growing regions, Geoscience Data Journal, n/a, https://doi.org/10.1002/gdj3.178, _eprint: https://onlinelibrary.wiley.com/doi/pdf/10.1002/gdj3.178, 2022.

Wang-Erlandsson, L., Bastiaanssen, W. G. M., Gao, H., Jägermeyr, J., Senay, G. B., van Dijk, A. I. J. M., Guerschman, J. P., Keys, P. W., Gordon, L. J., and Savenije, H. H. G.: Global root zone storage capacity from satellite-based evaporation, Hydrology and Earth System Sciences, 20, 1459–1481, https://doi.org/10.5194/hess-20-1459-2016, publisher: Copernicus GmbH, 2016.

Xiao, M., Gao, M., Vogel, R. M., and Lettenmaier, D. P.: Runoff and Evapotranspiration Elasticities in the Western United States: Are They Consistent With Dooge's Complementary Relationship?, Water Resources Research, 56, e2019WR026 719, https://doi.org/10.1029/2019WR026719, _eprint: https://onlinelibrary.wiley.com/doi/pdf/10.1029/2019WR026719, 2020.

Xiong, J., Yin, J., Guo, S., He, S., Chen, J., and Abhishek: Annual runoff coefficient variation in a changing environment: a global perspective, Environmental Research Letters, 17, 064 006, https://doi.org/10.1088/1748-9326/ac62ad, publisher: IOP Publishing, 2022.

Xu, D., Bisht, G., Sargsyan, K., Liao, C., and Leung, L. R.: Using a surrogate-assisted Bayesian framework to calibrate the runoff-generation scheme in the Energy Exascale Earth System Model (E3SM) v1, Geoscientific Model Development, 15, 5021–5043, https://doi.org/10.5194/gmd-15-5021-2022, publisher: Copernicus GmbH, 2022.

Yang, X., Yong, B., Ren, L., Zhang, Y., and Long, D.: Multi-scale validation of GLEAM evapotranspiration products over China via ChinaFLUX ET measurements, International Journal of Remote Sensing, 38, 5688–5709, https://doi.org/10.1080/01431161.2017.1346400, publisher: Taylor & Francis _eprint: https://doi.org/10.1080/01431161.2017.1346400, 2017.

Zaitchik, B. F., Rodell, M., Biasutti, M., and Seneviratne, S. I.: Wetting and drying trends under climate change, Nature Water, pp. 1–12, https://doi.org/10.1038/s44221-023-00073-w, publisher: Nature Publishing Group, 2023.

Zhang, Y., Pan, M., and Wood, E. F.: On creating global gridded terrestrial water budget estimates from satellite remote sensing, in: Remote Sensing and Water Resources, pp. 59–78, Springer, 2016.

Zhao, L., Xia, J., Xu, C.-y., Wang, Z., Sobkowiak, L., and Long, C.: Evapotranspiration estimation methods in hydrological models, Journal of Geographical Sciences, 23, 359–369, https://doi.org/10.1007/s11442-013-1015-9, 2013.